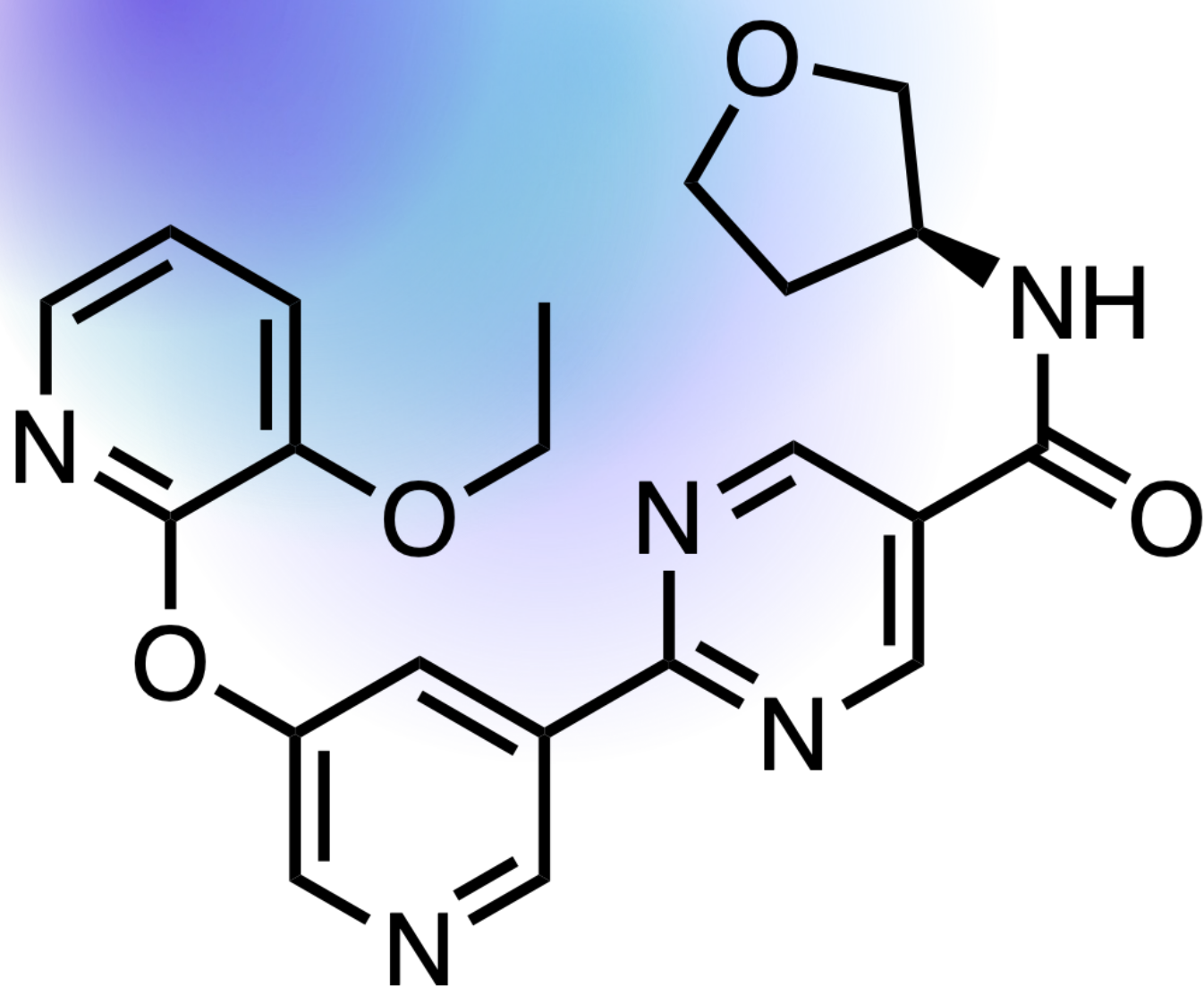


Small Molecules of the Month

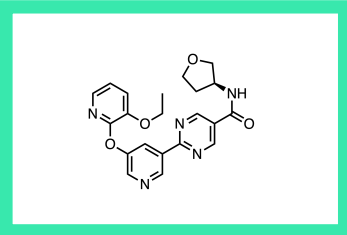
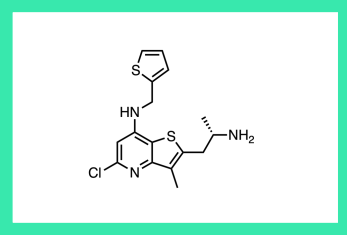
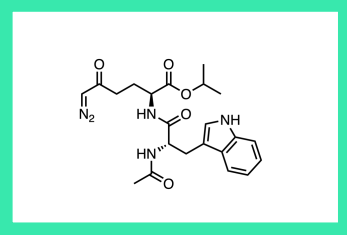
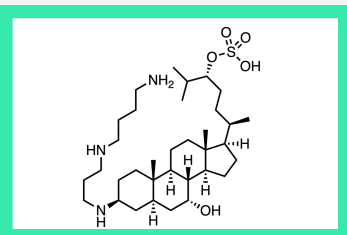
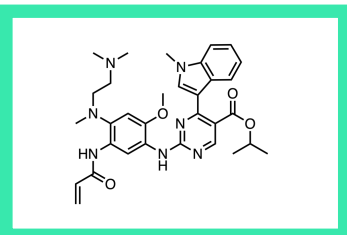
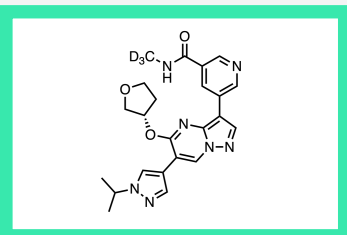
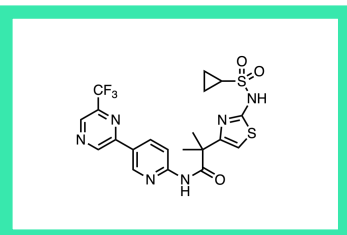
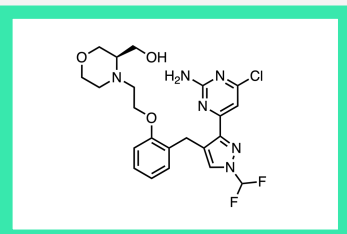
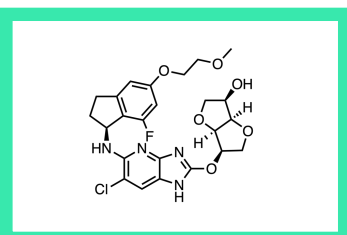
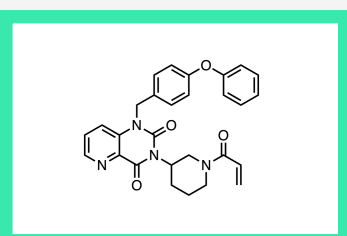
November 2022



drug
hunter

Table of Contents

November 2022

Page 3	ervogastat DGAT2	systemic, oral DGAT2 inhibitor	Ph. II for NASH with fibrosis	PFIZER, CAMBRIDGE, MA AND GROTON, CT	
Page 4	PTC258 mutant ELP1 pre-mRNA	oral ELP1 ex20 splicing modulator	rescues motor coordination in FD mouse model	MASS GENERAL / PTC THERAPEUTICS	
Page 5	sirpiglenastat glutamine antimetabolite	IV/SC glutamine antimetabolite prodrug	Ph. I/IIa in advanced solid tumors	JOHNS HOPKINS / DRACEN PHARMACEUTICALS	
Page 6	ENT-01 α -synuclein	oral α -synuclein aggregation inhibitor	completed Ph. IIb for PD + constipation	ENTERIN INC., PHILADELPHIA, PA	
Page 7	mobocertinib EGFR ex20 mutants	EGFR exon 20 mutant inhibitor, oral once-daily	FDA-approved for EGFR ex20+ NSCLC	ARIAD/TAKEDA, CAMBRIDGE, MA	
Page 9	compound 29 FGFR2/3	FGFR2/3 inhibitor	favorable PK profile in rats	INCYTE CORPORATION, WILMINGTON, DE	
Page 10	compound 27 CTPS1/2	CTPS1/2 inhibitor	in vivo anti- inflammatory activity in mice	SYGNATURE DISCOVERY, UK AND STEP PHARMA, FR	
Page 12	compound 14d β 2-AMPK	β 2-AMPK activator	in vivo efficacy in diabetic mouse model	SHIONOGI & CO., OSAKA, JP	
Page 14	TDI-11861 sAC	oral sAC inhibitor	intended for male contraception	TRI-I TDI/WEILL CORNELL MEDICINE, NY	
Page 15	EG-011 WASp	WASp activator	in vivo antitumor activity	INSTITUTE OF ONCOLOGY RESEARCH, CH	

November 2022

ervogastat

DGAT2

systemic, oral DGAT2 inhibitor

Ph. II for NASH with fibrosis (MIRNA)

opt. of liver-targeted candidate PF-06427878

J. Med. Chem., 02 November 2022

PFIZER, CAMBRIDGE, MA AND GROTON, CT

paper DOI: <https://doi.org/10.1021/acs.jmedchem.2c01200>

[View Online](#)

Toward a first-in-class DGAT2 inhibitor for the treatment of NASH.

Hepatic triglyceride (TG) accumulation is a symptom of non-alcoholic fatty liver disease (NAFLD), which can progress to non-alcoholic steatohepatitis (NASH), which is characterized by hepatocyte damage, inflammation and collagen deposits (fibrosis). NASH has been estimated to impact 3-5% of the global population, with up to 29% of these individuals developing cirrhosis within 10 years and 4-27% of these patients developing hepatocellular carcinoma. Despite significant research, there are currently no FDA-approved medications for this burgeoning global health crisis. Several targets and mechanisms to treat NASH are being evaluated, including diacylglycerol acyltransferase (DGAT) inhibition.

DGAT2 as a target. DGAT enzymes catalyze the esterification of diacylglycerol (DAG) in the final step of triglycerol biosynthesis in hepatocytes. DGAT1 is expressed in the intestine and resides in the endoplasmic reticulum (ER), whereas DGAT2 can be found in lipid droplets and the ER in the liver and adipose tissue. In the early 2000s, DGAT2 knock-down/inhibition by antisense nucleotides (ASOs), DGAT2 gene silencing or small molecules was demonstrated to decrease hepatic lipid levels. Both Eli Lilly (WO2016187384A1, WO2015077299A1) and Merck have demonstrated in vivo activity with small molecule DGAT2i programs. The most recent clinical studies involving DGAT include a study for an ASO, IONIS-DGAT2_{Rx} and studies for Pfizer's oral, liver-targeted small molecule PF-06427878, the starting point for this Molecule of the Month, ervogastat.

Mitigating clearance and a safety risk by addressing metabolic liabilities. Pfizer successfully demonstrated clinical proof-of-concept with PF-06427878, with substantially reduced liver fat and a good tolerability profile after ~2 weeks of treatment in healthy adults. However, its development was terminated following the Ph. I clinical trials due to CYP-mediated N- and O-dearylation and corresponding failure to achieve a reasonable and reliable efficacious clinical dose. PF-06865571/ervogastat was the result of a campaign to identify a neutral systemic candidate with improved pharmacokinetics (reduced clearance) and mitigated CYP-mediated metabolism relative to liver-targeted PF-06427878.

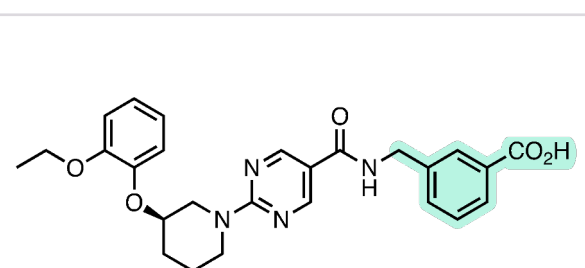
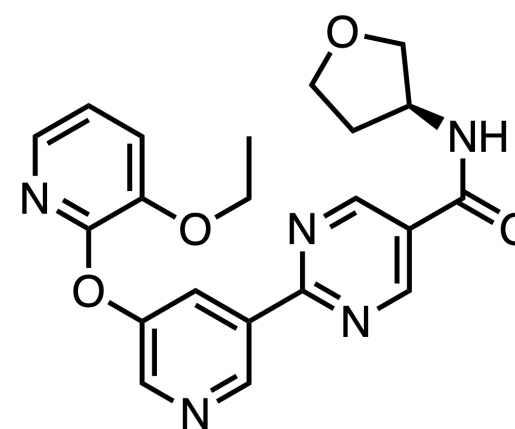
Mitigating clearance and a safety risk by addressing metabolic liabilities. Metabolite studies of PF-06427878 revealed CYP-mediated O-

deethylation of '7878 to the corresponding phenol, as well as oxidative diarylation to afford the corresponding piperidinol and potentially, a reactive quinone precursor in the form of a catechol. Removal of the liver-targeting, carboxylic acid OATP 1B1/1B3 transporters recognition element led to neutral systemic molecule "compound 1." To mitigate the reactive metabolite safety risk, the piperidine and masked catechol rings of "compound 1" were replaced with substituted pyridines, resulting in "compound 3" with reduced clearance (HLM CL_{int,app} = 12 vs. 141 μL/min/mg), comparable potency (DGAT2 IC₅₀ = 6.6 vs. 7.9 nM) and favorable PK properties (LogD = 2.0 vs. 2.8). The team sought further to improve the projected half-life of ~2h by modifying the amide, informed by previous studies that this moiety had flat SAR. Replacing the dimethylpropyl amide with a tetrahydrofuran mitigated possible oxidative metabolism of that primary alcohol and increased the projected half-life to ~5h for "compound 6"/PF-06865571/ervogastat, enabling human BID dosing. In vitro metabolite studies of ervogastat in human, rat and monkey hepatocytes confirmed a lack of O-dearylation.

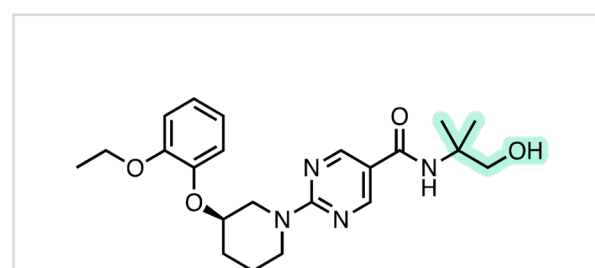
Other notable pharmacology. Despite having a monosubstituted pyridine, the molecule did not show significant reversible CYP inhibition (lowest CYP IC₅₀ = 7.8 μM for 2C9). This was attributed to the low overall lipophilicity of the molecule and the low pKa (2.5) of the electron-deficient pyridine. Interestingly, as was observed with the previous imidazopyridine series containing PF-06424439 and parent compound PF-06427878, this molecule is more potent in hepatocytes than in the biochemical DGAT assay, though it is not liver-targeted. No explanation was provided for the left-shift in biochemical vs. cell potency.

Back into the clinic. The efficacy and safety of ervogastat as a single agent and in combination with acetyl-coenzyme A carboxylase inhibitor (ACCi) clesacostat (PF-05221304) is showing promise in reducing hepatic steatosis in early Ph. II clinical trials (NCT04321031). Ervogastat is dosed 25 mg to 300 mg BID. This study is for the treatment of metabolic interventions to resolve non-alcohol steatohepatitis with fibrosis (MIRNA) and has an estimated completion of Q1 2024. The FDA granted Fast Track designation to this combination therapy on May 26, 2022.

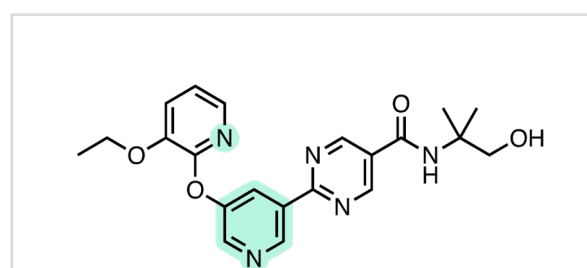
Patents. "Diacylglycerol acyltransferase 2 inhibitors": WO2018033832A1 (2/22/2018), US20210309646A1 (10/7/2021)



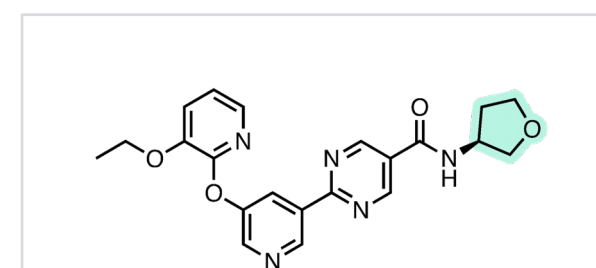
PF-06427878
DGAT2 IC₅₀ = 92 nM
HLM CL_{int,app} = 9 μL/min/mg
liver transporter substrate



"compound 1"
DGAT2 IC₅₀ = 7.9 nM
HLM CL_{int,app} = 121 μL/min/mg
neutral systemic distribution



"compound 3"
DGAT2 IC₅₀ = 6.6 nM
HLM CL_{int,app} = 14 μL/min/mg
HHEP CL_{int,app} = 8 μL/min/million cells



ervogastat
(PF-06865571, "compound 6")
DGAT2 IC₅₀ = 17.2 nM
HHEP CL_{int,app} = 3.9 μL/min/million cells

November 2022

PTC258

mutant ELP1 pre-mRNA

oral ELP1 ex20 splicing modulator
rescues motor coordination in FD mouse model
opt. from natural product from 1K compd screen
bioRxiv, 04 November 2022
MASS GENERAL / PTC THERAPEUTICS
paper DOI: <https://doi.org/10.1101/2022.11.04.515198>

[View Online](#)

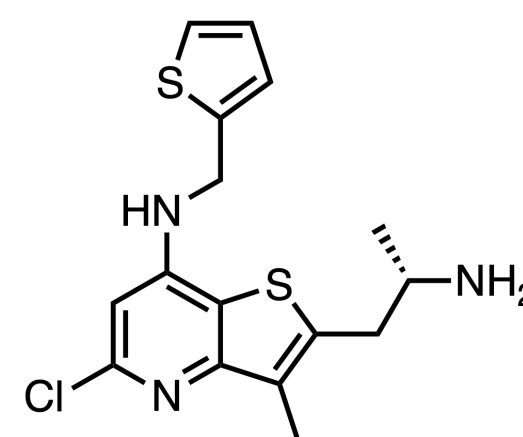
An oral, brain-penetrant splicing modulator targeting ELP1.

[Incorrect splicing](#) of the [Elongator complex protein 1](#) (ELP1) gene causes [Familial Dysautonomia](#) (FD), a neurodegenerative disease that results in uncoordinated movement, blindness through retinal degeneration, and risk of unexplained sudden death, among other symptoms. A single T-to-C nucleotide change in the 5' splice site of ELP1 [intron 20](#) leads to [skipping of ELP1 exon 20](#) and a reduction in ELP1 protein in the CNS and PNS. There are no effective treatments for FD, though [antisense oligonucleotides](#), modified [exon-specific U1 small nuclear RNAs](#), and [splicing modulator compounds](#) have been investigated. PTC258 is an oral, brain-penetrant small molecule that increases functional ELP1 protein levels in the CNS by correcting splicing of mutant ELP1 pre-mRNA.

Discovery and 30,000x potency improvement from a natural product.

The starting point and plant growth factor natural product, kinetin (EC_{2x} ELP1 = 10 μM) was [reported in 2004](#). A panel of 1040 bioactive compounds from the NINDS Custom Collection [was screened](#) using an assay that measures the ratio of WT:MU FD IKBKAP mRNA splice products in a lymphoblast cell line. A team including scientists at Mass General and PTC Therapeutics as part of the [NIH Blueprint Neurotherapeutics Network](#) developed [assays for ELP1 splicing](#) and identified a ~30x more potent kinetin analogue, [BPN15477](#).

Introduction of an amine-containing substituent at the 2-position of the pyrrole provided a significant gain in potency (e.g. PTC102). The stereochemistry of the amine was important in this case, favoring the (S)-enantiomer, supporting a target-based mechanism. Further optimization was achieved through the replacement of the pyrrolopyrimidine ring system with a more lipophilic thienopyridine and the sidechain pyridine with a more

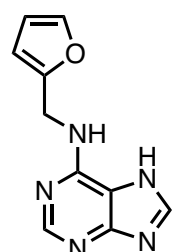


lipophilic thiophene (PTC258). The resulting picomolar compound is remarkably atom-efficient, which likely contributes to its favorable absorption and brain-penetrating properties.

Efficacy in nursing pups via lactation, and functional improvements in maturing animals.

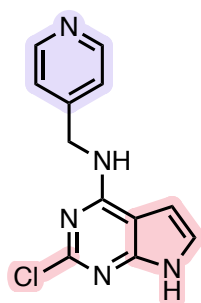
In vivo testing of PTC258 was performed in a TgFD9 transgenic mouse model that carries the human ELP1 gene with the major FD splice mutation. Special chow was formulated to deliver each mouse dam either 3 mg/kg/d, 6 mg/kg/d, 12 mg/kg/d, or 24 mg/kg/d. An increase in full-length ELP1 transcript and a >5x increase in functional ELP1 protein in the brain, trigeminal nerve, liver, and muscle were observed in a dose-dependent manner in pups, with maximum effect at 12 mg/kg/d (0.008% PTC258 in chow) fed to the dams. Continued treatment of the mice resulted in a functional improvement in motor coordination at six months of age. PTC258 also dose-dependently prevented retinal degeneration in the FD mouse model. No adverse effects or weight loss were reported, even at the highest tested dose concentration.

A program to watch. While additional profiling and safety data is needed, given the lack of existing options for FD patients, the initial preclinical data is encouraging. Scientifically, the molecule represents an interesting proof-of-concept for a splicing modulator with activity in the CNS and with efficacious exposures through lactation. PTC does not appear to have a disclosed FD asset in its pipeline yet, but PTC258 and other thieno(3,2-b)pyridin-7-amine compounds for regulation of transgene expression and familial dysautonomia treatment were described in the patents [WO202220471A1](#) and [WO2020167628A1](#). The US patent [US20220135586A1](#) is still pending.



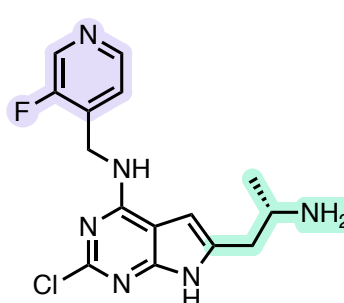
kinetin

EC_{2x} ELP1 prot. = 10,000 nM



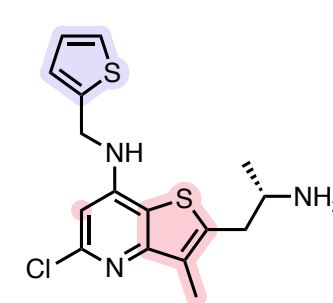
BPN15477

EC_{2x} FL ELP1 mRNA = 190 nM
EC_{2x} ELP1 prot. = 340 nM
mAUC = 3.1 μg.h/mL



PTC102

EC_{2x} FL ELP1 mRNA = 7 nM
EC_{2x} ELP1 prot. = 9 nM
mAUC = 0.3 μg.h/mL



PTC258

EC_{2x} FL ELP1 mRNA = 0.2 nM
EC_{2x} ELP1 prot. = 0.3 nM
mAUC = 4.2 μg.h/mL

November 2022

sirpigenastat

glutamine antimetabolite

IV/SC glutamine antimetabolite prodrug

Ph. I/IIa in advanced solid tumors

dual prodrug of natural product

Sci. Adv., 16 November 2022

JOHNS HOPKINS / DRACEN PHARMACEUTICALS

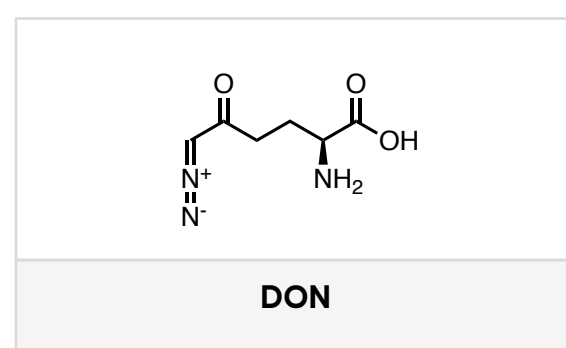
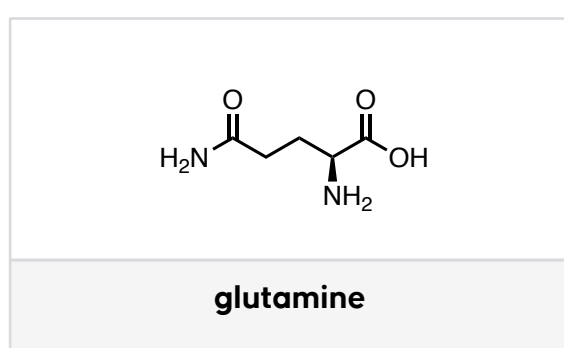
paper DOI: <https://doi.org/10.1126/sciadv.abq5925>

[View Online](#)

A first-in-class diazo-prodrug for the treatment of solid tumors.

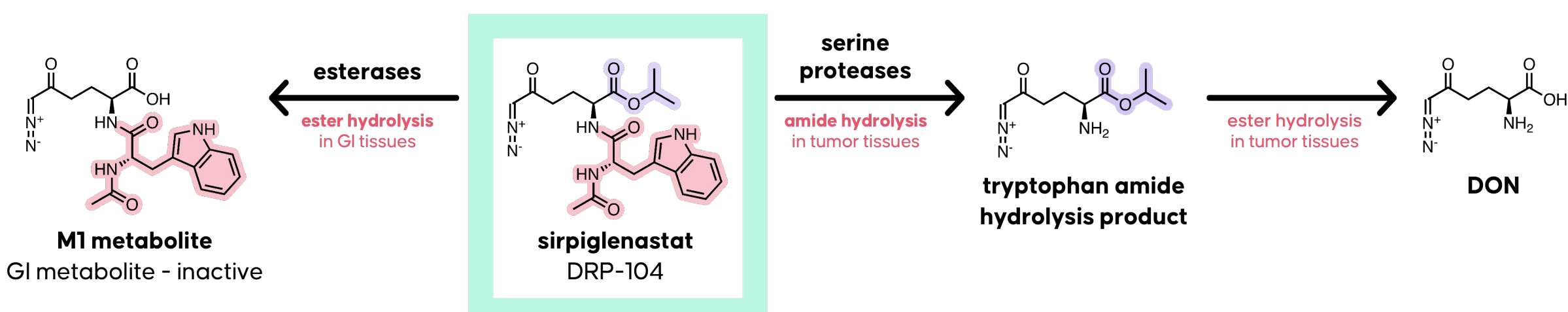
[Sirpigenastat \(DRP-104\)](#) (Johns Hopkins/Dracen Pharmaceuticals) is a dual prodrug of [6-diazo-5-oxo-L-norleucine \(DON\)](#), a diazoketone-based glutamine irreversible antagonist used to suppress cancer cell metabolism. [Rapidly growing cancer cells](#) depend on [glutamine](#) as an energy source via the tricarboxylic acid (TCA) cycle, as well as a carbon and nitrogen source for biosynthesis and cellular homeostasis. Thus, approaches to blocking glutamine uptake or [metabolism](#) (e.g. glutaminase inhibitors such as [telaglenastat](#) (Calithera, [Ph. I/II](#))) have been investigated. Although DON itself demonstrated promising [preclinical](#) and [clinical](#) efficacy, the program was terminated due to [dose-limiting gastrointestinal \(GI\) toxicities](#).

As a dual prodrug that is selectively activated in tumor cells and deactivated in GI tissues, sirpigenastat has a significantly better therapeutic window than DON. It has impressive preclinical efficacy, and as a monotherapy leads to durable anti-tumor immunity in mouse models in part by [enhancing the function of CD8+ T cells](#). Sirpigenastat is currently being evaluated in a Ph. I/IIa ([NCT04471415](#)) study for the treatment of advanced solid tumors as a single agent and in combination with atezolizumab in metastatic NSCLC. It also received an [FDA Fast Track designation](#) in October 2020 for the treatment of non-small cell lung cancer (NSCLC) with KEAP1, NFEL2 and/or STK11 mutations.



Discovery and mechanism of action of 6-diazo-5-oxo-L-norleucine (DON).

DON was [first isolated](#) as an antibiotic from an unidentified *Streptomyces* species in 1956. It is structurally similar to glutamine and selectively inhibits many enzymes which utilize glutamine as a substrate. In human kidney-type (KGA), the α -diazoketone of DON is [activated by a proton transfer](#) from a serine residue,



generating a cation that rapidly alkylates Ser286 with concomitant N_2 release. This covalent bond with the Ser286 residue in the catalytic pocket was confirmed by X-ray crystal structure (PDB:[4O7D](#)), along with several stabilizing hydrogen bonds or hydrophobic contacts with key residues. Given glutamine's role in numerous metabolic pathways, this leads to a broad shift across the metabolome, which is empirically beneficial for cancer treatment.

Sirpigenastat is activated to release DON in tumors but forms an inert metabolite in GI tissues.

In tumor cells, the tryptophan amide is hydrolyzed first by serine proteases before ester hydrolysis, liberating active DON ($EC_{50} = 4.0 \mu M$). In contrast, in GI tissues, the ester is cleaved first by esterases, resulting in an inactive carboxylic acid metabolite, M1, that does not release DON. Experiments with serine protease inhibitor [Pefabloc](#) and [dual protease/esterase inhibitor PMSF](#) were used to verify this hypothesis. In a mouse tumor model, DON levels were 6-fold higher in the tumor ($AUC_{0-t} = 4.1 \text{ nmol hr/g}$) than in plasma ($AUC_{0-t} = 0.7 \text{ nmol hr/g}$) and 11-fold higher than in the intestinal tissue ($AUC_{0-t} = 0.4 \text{ nmol hr/g}$). While both DON and sirpigenastat led to complete regressions in a tumor model, sirpigenastat was visibly less toxic to the GI, in contrast to the widespread ulceration seen after DON dosing.

Durable responses to monotherapy. Mice that were initially cured with sirpigenastat monotherapy were implanted with the same tumors after 60 days, and the mice completely rejected the tumors, suggesting development of immunologic memory, mediated by T cells. While the mechanism is not clear, enabling immune-mediated tumor clearance would be a valuable property if confirmed in humans.

12 more years of patent coverage: Sirpigenastat and other glutamine antagonists used to treat oncological, immunological, and neurological diseases have been disclosed in the patent [WO2019071110A1](#). The US patent [US20190216757A1](#) was granted to Johns Hopkins University in November 2020 and is valid until July 2036.

November 2022

ENT-01

α -synuclein

oral α -synuclein aggregation inhibitor
completed Ph. IIb for PD + constipation
natural product

Sci. Adv., 16 November 2022

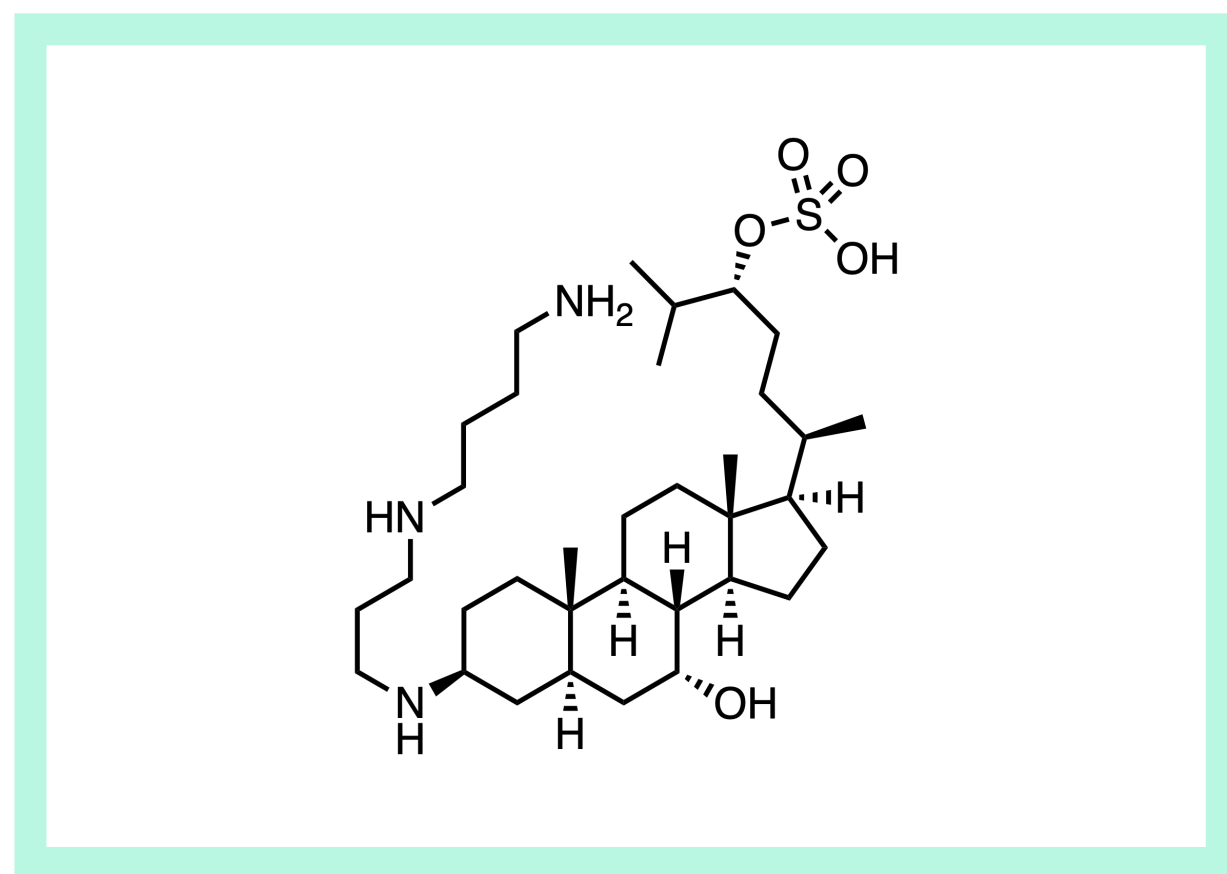
ENTERIN INC., PHILADELPHIA, PA

paper DOI: <https://doi.org/10.7326/m22-1438>

[View Online](#)

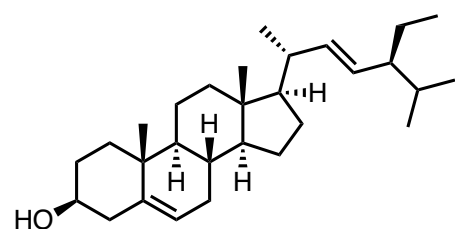
An old molecule and an old target come together. Squalamine was [originally discovered](#) in 1993 as an antimicrobial from the liver of the dogfish shark. It's had a long and interesting history, investigated by Magainin/Genaera as a [Ph. II antiangiogenic drug candidate for cancer](#) and as a [Ph. III ophthalmic candidate](#) for macular degeneration. One of the scientists from Magainin, [Michael Zasloff](#), is now the co-founder and CSO of Enterin, a company trying to develop squalamine as an oral, [non-systemic](#) drug for Parkinson's disease.

The Parkinson's disease hypothesis. [\$\alpha\$ -Synuclein aggregation](#) is a hallmark of Parkinson's disease (PD) and other [synucleinopathies](#). α -Synuclein aggregates are neurotoxic but [targeting \$\alpha\$ -Synuclein](#) directly is challenging due to its relatively small size (14 kDa), [unclear but important endogenous role](#), and high concentrations (50 μ M) in neuronal synapses. PD is associated with α -synuclein aggregation in and functional disturbance of the enteric neurons of the GI tract, resulting in constipation as a common problem in PD patients. Constipation [affects >60% of PD patients](#) and is mostly chronic, severe, and non-responsive to standard treatments. ENT-01 competes with α -synuclein for binding with lipid membranes, inhibiting aggregation and toxicity of α -synuclein oligomers in [neurons](#) and [animal models](#). This novel approach of addressing α -synuclein in the enteric system could improve signaling in the gut-brain axis and prevent accumulation of α -synuclein in the CNS, potentially slowing progression of neurological symptoms.

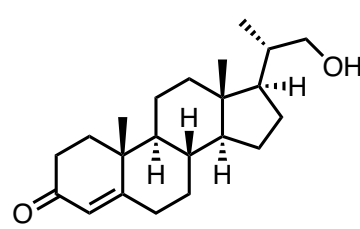


Clinical activity in Parkinson's patients. While the cellular MoA has not been confirmed in patients, initial clinical data is promising. ENT-01 completed a Ph. IIb study in PD + constipation (KARMET, [NCT03781791](#), n=150) in which it met both its primary and secondary bowel endpoints for constipation. Results from small subgroups of patients suggested that ENT-01 might also improve psychosis and dementia. The [main side effects](#) of nausea and diarrhea appear to be manageable. According to [Enterin](#), ENT-01 will begin Ph. IIa trials in PD + psychosis and PD + dementia in 2023 and is being evaluated for a Ph. II trial in autism. While one could be reasonably skeptical about the mechanism of constipation relief with a marine natural product in Parkinson's disease given the challenge of finding effective therapeutics in PD so far, it is an interesting hypothesis to watch given the preclinical support and early clinical data.

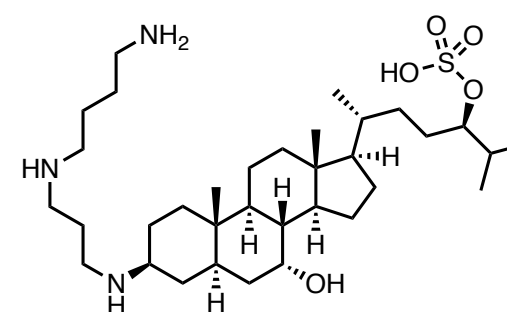
An example of a natural product candidate from semisynthesis. While squalamine was originally isolated from animals ([100 mg per 500 kg of dogfish shark liver](#)), synthetic routes have been needed to supply it for clinical studies. A [1995 route](#) developed by Magainin involves 15 steps from the abundant plant sterol, [stigmasterol](#). The [current route](#) appears to start from progesterone bisnoralcohol, obtained from soybean sterol fermentation.



stigmasterol



progesterone bisnoralcohol



squalamine phosphate

November 2022

mobocertinib

EGFR ex20 mutants

EGFR exon 20 mutant inhibitor, oral once-daily

FDA-approved for EGFR ex20+ NSCLC

from cellular screening + SBDD

Bioorg. Med. Chem. Lett., 21 November 2022

ARIAD/TAKEDA, CAMBRIDGE, MA

paper DOI: <https://doi.org/10.1016/j.bmcl.2022.129084>

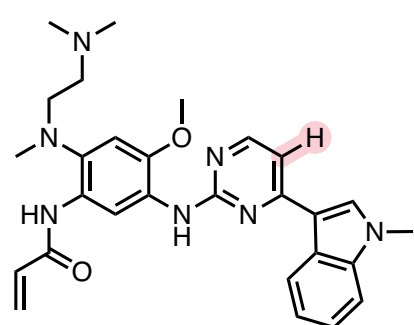
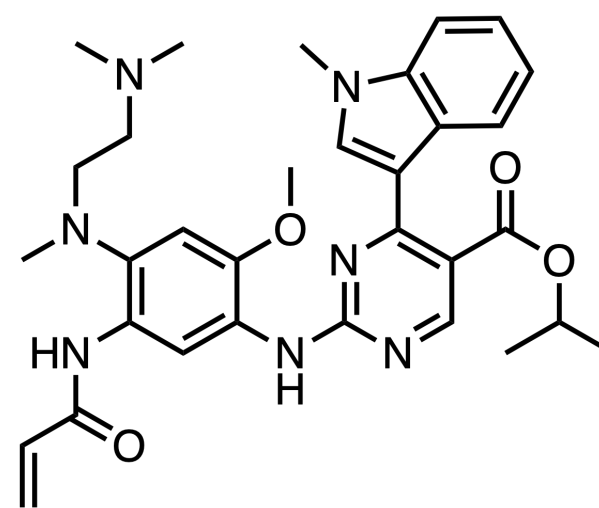
[View Online](#)

The first approved EGFR exon 20 mutant inhibitor. While there are now [three generations of EGFR inhibitors](#) approved, patients harboring the common EGFR exon 20 insertion resistance mutations haven't responded well to previously approved drugs. This mutation class makes up [4–12% of all mutant EGFR-positive NSCLC cases](#) and has the highest incidence beyond the most common EGFR mutations, illustrating this unmet medical need. Mobocertinib (Exkivity) is a Breakthrough Therapy that we highlighted as a [Molecule of the Month in February 2021](#) and was recently approved for NSCLC as the [first EGFR exon 20 inhibitor](#). Details around its discovery have finally been disclosed, warranting this update.

EGFR exon 20 mutants are hard to drug. Unlike active site mutations like EGFR T790M, [EGFR exon 20 mutants have active sites that are very similar to WT EGFR](#), which limits treatment options due to GI toxicities and rashes. Additionally, unlike other mutants like L858R and exon 19 deletions, [which are highly sensitive to ATP-competitive first-generation EGFR inhibitors due to reduced ATP affinity](#), exon 20 insertion mutants like D770_N771insNPG (NPG) activate EGFR [without reducing ATP affinity or increasing affinity for first-generation inhibitors](#). Furthermore, EGFR exon 20 insertions are heterogeneous, caused by the addition of 1–7 amino acids between residues 762 and 774 of EGFR. There are [122 Exon 20 mutations](#) identified so far, making up 1–10% of all EGFR mutations. An effective drug needs to have activity against a broad spectrum of these mutant proteins

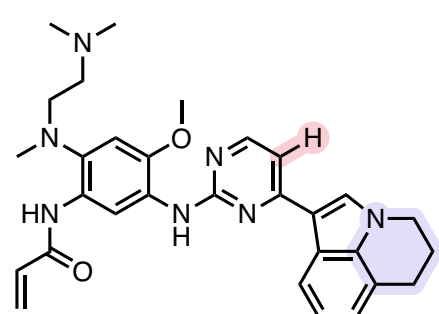
while maintaining selectivity against WT EGFR, a challenge given the distance of the insertion site to the active site.

A cell-based search for selectivity. An [exon 20 mutant cell line](#) of Ba/F3 cells expressing NPG was used to screen for activity and selectivity against WT EGFR. It was important to measure cell-based activity, as mutant forms of EGFR can have [different sensitivities to inhibitors in cells](#) due to differences in ATP affinity relative to WT EGFR. Testing libraries of EGFR inhibitors, including approved drugs, led to the finding that osimertinib not only had an IC_{50} of 50 nM against the mutant cell line, but also had a ~6x selectivity window relative to WT EGFR, based on a cellular phosphorylation assay. Given the homology between the WT EGFR active site and EGFR exon 20 mutant active sites, a WT EGFR homology model was used to guide compound design due to the lack of published EGFR exon 20 x-ray co-crystal structures at the onset of the campaign. X-ray co-crystal structures of inhibitors with WT EGFR were routinely gathered to update their models. Because it was reported that the demethylation of the indole was a [major metabolic liability of osimertinib](#), tricyclic analogs were pursued first to mitigate dealkylation and improve potency.



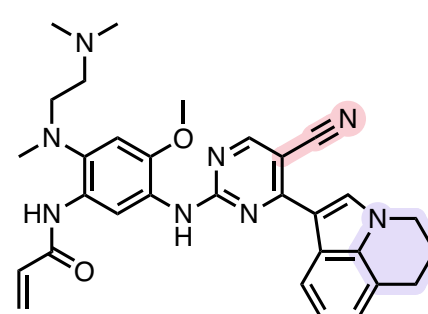
osimertinib

exon 20 mutant (NPG) IC_{50} = 53 nM
WT EGFR (p-EGFR) cell IC_{50} = 300 nM
selectivity ~5.7x



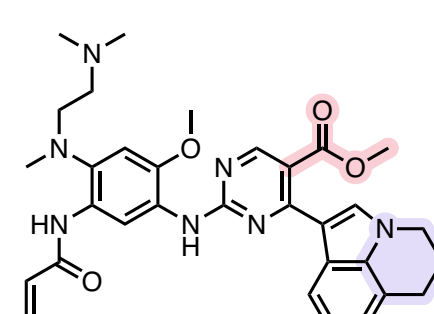
compound 8a

exon 20 mutant (NPG) IC_{50} = 54 nM
WT EGFR (p-EGFR) cell IC_{50} = 405 nM
selectivity ~7.5x



compound 12a

exon 20 mutant (NPG) IC_{50} = 4.0 nM
WT EGFR (p-EGFR) cell IC_{50} = 35 nM
selectivity ~8.8x



compound 12d

exon 20 mutant (NPG) IC_{50} = 6.6 nM
WT EGFR (p-EGFR) cell IC_{50} = 40 nM
selectivity ~6.0x

November 2022

mobocertinib

EGFR ex20 mutants

EGFR exon 20 mutant inhibitor, oral once-daily

FDA-approved for EGFR ex20+ NSCLC

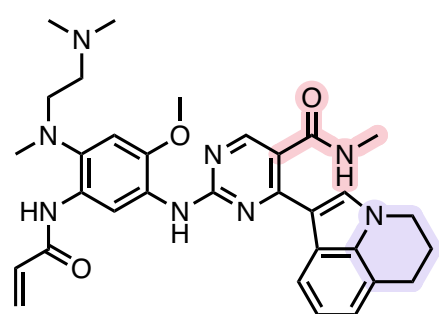
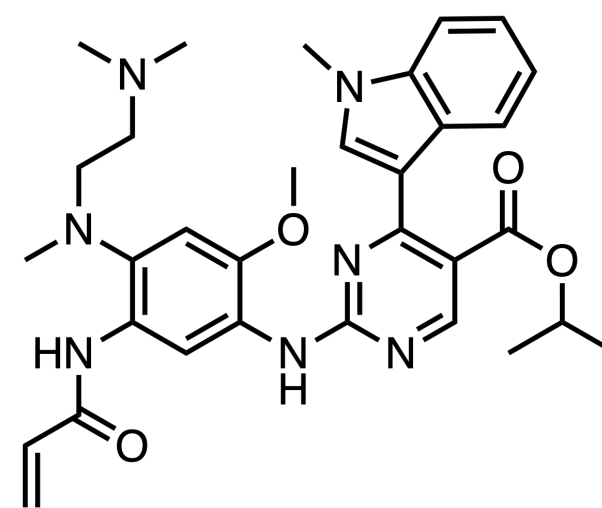
from cellular screening + SBDD

Bioorg. Med. Chem. Lett., 21 November 2022

ARIAD/TAKEDA, CAMBRIDGE, MA

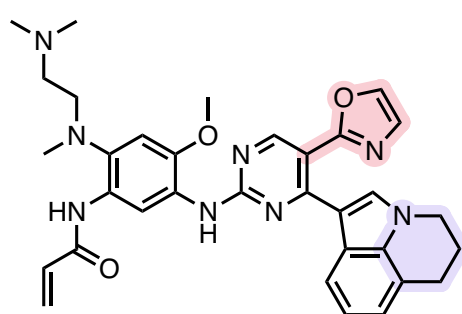
paper DOI: <https://doi.org/10.1016/j.bmcl.2022.129084>

[View Online](#)



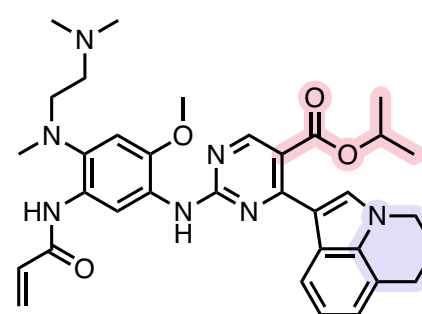
compound 12i

exon 20 mutant (NPG) IC_{50} = 6.2 nM
WT EGFR (p-EGFR) cell IC_{50} = 15 nM
selectivity ~2.4x



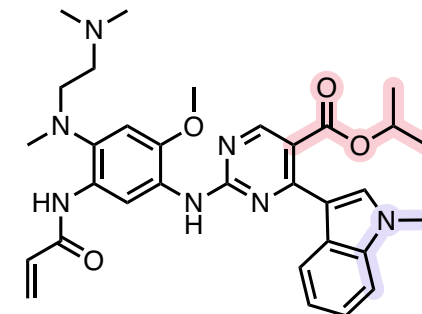
compound 12g

exon 20 mutant (NPG) IC_{50} = 39 nM
WT EGFR (p-EGFR) cell IC_{50} = 147 nM
selectivity ~3.8x



compound 12f

exon 20 mutant (NPG) IC_{50} = 6.6 nM
WT EGFR (p-EGFR) cell IC_{50} = 39 nM
selectivity ~5.9x



mobocertinib (21c)

exon 20 mutant (NPG) IC_{50} = 4 nM
WT EGFR (p-EGFR) cell IC_{50} = 31 nM
selectivity ~7.8x

A rare example of a non-prodrug ester. Compounds with hydrogen bond acceptors at C5 were generally more potent than “compound 8a”, likely due to their ability to hydrogen bond with Cys775 and Thr854 in the binding site. Nitrile “12a” and ester “12d” were more potent and offered selectivity over the WT than the corresponding amide (“12g”). Methyl ester “12d” surprisingly had promising rodent PK, prompting exploration of ester bioisoteres. Unfortunately, most alternatives such as oxazole “12i” maintained good properties, but had lower selectivities against WT. To improve oral exposures in mice with wider selectivity over WT, the team returned to the *N*-methylindole, eventually discovering isopropyl ester “21c” (mobocertinib). This molecule has marginally higher potency and selectivity than its tricyclic counterpart, “compound 12f”. Increasing the ester group size to butyl derivatives demonstrated reduced activity. Interestingly, significantly greater

oral exposures were observed with mobocertinib in rats than mice, yet another example of an approved drug with a species PK disconnect, a common headache for teams at this preclinical stage.

Binding mode. X-ray crystal structures were eventually obtained of mobocertinib in complex with WT (PDB: [7T4I](#)) and exon 20 mutant EGFR/V948R (PDB: [7T4I](#)) and confirmed hydrogen bonding of the ester with Thr854 in both proteins. However, the ester interacts with a back pocket water molecule in the mutant version and instead of interacting with Cys775 in the WT protein. This is a surprising example of an ester-containing drug that is not facilitating a prodrug mechanism-of-action. Esters are generally avoided by medicinal chemists given their rapid metabolism by esterases in plasma and tissues.

A first approval for EGFR exon 20 mutants. Accelerated approval for NSCLC in combination with a companion diagnostic was granted [based on 114 patients](#) (NCT02716116) with an ORR of 28% and median duration of response of 17.5 months. While a controlled, head-to-head study is needed, the data is promising in a setting with very limited options. Unfortunately, mobocertinib does carry risk of grade >3 diarrhea (22%), possibly related to WT EGFR inhibition,

though risk of grade >3 rash is limited (~2%). In humans, mobocertinib succinate has sufficient oral PK ($F\%$ = 37, $t_{1/2}$ = 18 h) for once daily dosing (160 mg). The order of magnitude greater potency of the molecule for exon 20 mutations over osimertinib likely allows it to show efficacy at a comparable dose (80 mg QD for osimertinib).

A black box warning for unexpected QTc prolongation. The drug also carries a black box warning for QTc prolongation, including TdP, requiring monitoring of QTc and electrolytes prior to and during treatment. The QTc risk also requires patients to avoid drugs that can prolong QTc due to drug-drug interactions (CYP3A inhibitors). In a 250 patient subset with echocardiograms (ECGs), 1.2% had a QTc interval >500 msec and 11% had change-from-baseline of >60 msec. Grade 4 TdP was observed in 1 patient (0.4%). While the molecule contains a basic amine and osimertinib is a known [hERG inhibitor](#) (IC_{50} = 690 nM), mobocertinib and its active metabolites are not significant hERG inhibitors (IC_{50} >5 μ M) and [no cardiac effects were seen preclinically in dogs](#). The reason for the discrepancy is [unknown](#).

What's next. Future generations of EGFR-targeting molecules could differentiate on either efficacy (e.g., resistance, brain metastases) or tolerability (e.g., selectivity vs. WT, cardiac safety). Several small molecules including [poziotinib](#) (Spectrum), [zipalertinib](#) (TAS6417, [Cullinan Oncology/Taiho](#)) and [sunvozertinib](#) (DZD9008, [Dizal](#)) are currently in clinical trials, which appear to be predominantly ATP-competitive Type I inhibitors based on their structures. Notably, Blueprint Medicines recently acquired a brain-penetrant exon 20 inhibitor [LNG-451](#) (BLU-451) from Lengo Therapeutics, which appears to have been taken into development.

Patent. “Heteroaryl compounds for kinase inhibition” [WO2015195228A1](#) (23 Dec 2015).

November 2022

compound 29

FGFR2/3

FGFR2/3 inhibitor

favorable PK profile in rats

opt. from HTS + SBDD & scaffold hopping

J. Med. Chem., 10 November 2022

INCYTE CORPORATION, WILMINGTON, DE

paper DOI: <https://doi.org/10.1021/acs.jmedchem.2c01366>

[View Online](#)

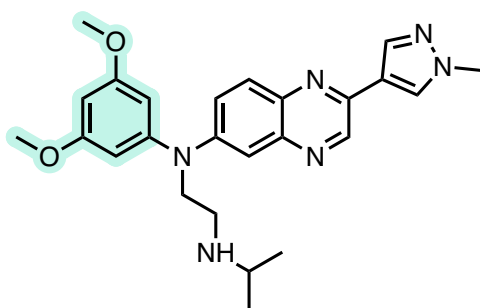
Tackling FGFR mutation resistance and FGFR1-mediated hyperphosphatemia toxicity through isoform-selective FGFR2/3 inhibition. “Compound 29” is an ATP-competitive fibroblast growth factor receptor (FGFR) 2/3 inhibitor with subnanomolar potency. FGFR is a receptor tyrosine kinase (RTK) involved in cell differentiation, proliferation, migration and survival. Aberrations in the *FGFR1-4* gene are related to oncogenesis and found in 5-10% of all human cancers, with a higher incidence of 10-30% in urothelial carcinoma and intrahepatic cholangiocarcinoma. FGFR1-3 inhibitors [erdafitinib](#) (Balversa), [pemigatinib](#) (Pemazyre), and [infigratinib](#) (Truseltiq) were FDA-approved in 2019-21, but clinical resistance has been reported due to [gatekeeper \(GK\) mutations](#) FGFR2^{V564I/L/M/F} or FGFR3^{V555I/L/M/F} such that the [3,5-dimethoxyphenyl group](#) can no longer reside in the hydrophobic pocket of the ATP-binding site. Even further, it has been shown that FGFR1 isoform inhibition leads to treatment-related toxicity due to [hyperphosphatemia](#). The FGFR1-4 inhibitor [futibatinib](#) (Lytgobi), with its recent [FDA-accelerated approval](#), alternately binds to the P-loop of the FGFR kinase domain, but still had a [81.2% incidence of hyperphosphatemia](#) in Ph. I dose-expansion trial patients. “Compound 29” was the result of a campaign to address the increasing FGFR mutant resistance and undesired on-target toxicity.

HTS for FGFR3-selective chemistry starting point. High-throughput screening focused on a starting point with potent FGFR3 activity (WT and mutant), but also selectivity against FGFR1. These efforts led to the discovery of “compound 4” which contains a unique imidazo[1,2b]pyridazine core not shared with the first-generation pan-FGFR (1-3) inhibitors.

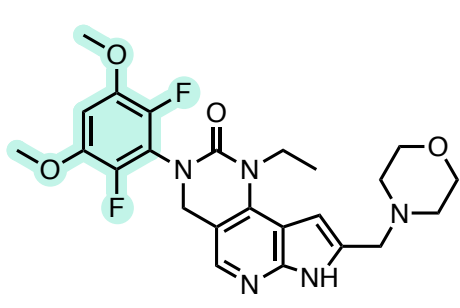
SBDD and scaffold hopping to improve FGFR isoform & kinase selectivity. SAR investigations revealed that the *N*-methylamide of “compound 4” was critical for the >10-fold selectivity for FGFR3 (WT and V555L mutant) over FGFR1, and the nicotinamide replacement of the phenyl ring in this position dramatically improved kinase selectivity, mitigating possible off-target toxicity. Analysis of “compound 9” docked in the ATP-binding site of FGFR3 (PDB:4K33) revealed hydrogen bonding of the *N*-methylamide carbonyl with Lys508 and that the *N*-methyl group extended past the GK Val555 residue. Even further, the proximity of the isopropoxy group in the lower hinge region to Asn562 inspired the team to install a hetero-cycloalkyl ring instead that might engage with the asparagine in hydrogen bonding. Correspondingly, a (*S*)-tetrahydrofuran replacement afforded “compound 19” with subnanomolar potency for FGFR3 and >30-fold selectivity over FGFR1.

Deuteration to avoid CYP3A4 inhibition. To mitigate the single-digit micromolar inhibition of CYP3A4, the *N*-methyl amide was replaced with the *N*-CD₃ congener, resulting in a drastically reduced in vitro clearance of 0.5 L/h/kg for “compound 29” over the non-deuterated version (1.0 L/h/kg) and >25 μM IC₅₀ for CYP3A4. These results indicated that [N-demethylation](#) of the amide was likely the culprit for the CYP metabolism.

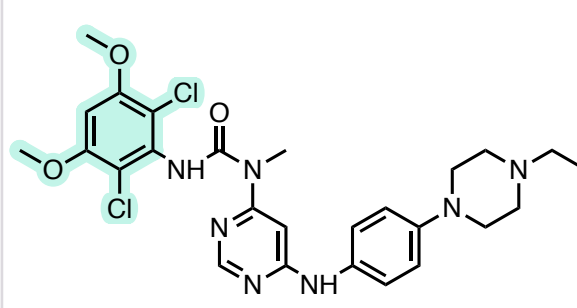
Current preclinical profile. To improve cell permeability, the basic imidazo[1,2b]pyridazine was replaced with a pyrazolo[1,5-*a*]pyrimidine and an isopropyl group replaced the pyrazole *N*-methyl group. These efforts resulted in “compound 29” with nanomolar activity in cell and whole blood assays (TEL-FGFR3-BA/F3 IC₅₀ = 5.5 nM, WB IC₅₀ = 177 nM), high permeability (Caco-2 = 2.0 × 10⁻⁶ cm/s), good solubility (FASSIF/SGF = 18/679 μg/mL), >100-fold kinase selectivity in an in-house panel, as well as low clearance (HBF = 35%) with moderate half-life (1.7h), good exposure (AUC = 5108 nM-h), and high bioavailability (F% = 82) in rat PK studies.



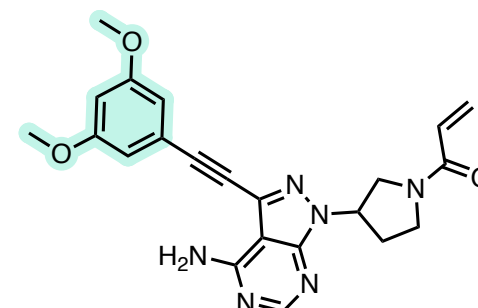
erdafitinib
FGFR2/3-mutant
urothelial carcinoma



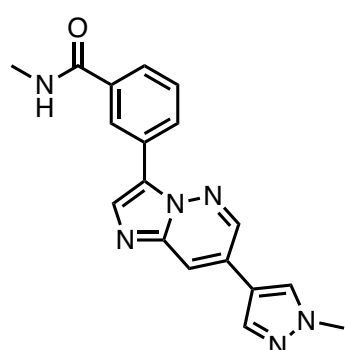
pemigatinib
FGFR2-mutant
cholangiocarcinoma



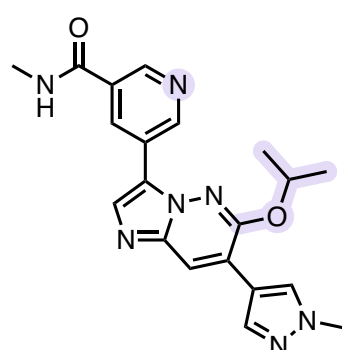
infigratinib
FGFR2-mutant
cholangiocarcinoma



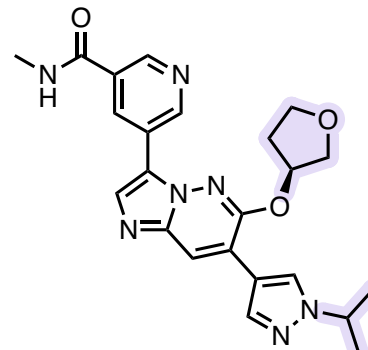
Futibatinib
FGFR2-mutant intrahepatic
cholangiocarcinoma



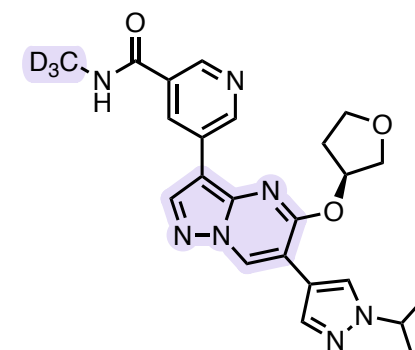
compound 4
FGFR3 IC₅₀ = 68 nM
FGFR3^{V555L} IC₅₀ = 22 nM
FGFR1 IC₅₀ = 918 nM



compound 9
FGFR3 IC₅₀ = 54 nM
FGFR1 IC₅₀ = 365 nM



compound 19
FGFR3 IC₅₀ = 0.9 nM
FGFR1 IC₅₀ = 30 nM
BA/F3 IC₅₀ = 15 nM



compound 29
FGFR3 IC₅₀ = 0.5 nM
FGFR1 IC₅₀ = 21 nM
BA/F3 IC₅₀ = 5.5 nM

November 2022

compound 27

CTPS1/2

CTPS1/2 inhibitor

in vivo anti-inflammatory activity in mice

in-house HTS of 240K library + opt.

J. Med. Chem., 30 November 2022

SYGNATURE, UK AND STEP PHARMA, FR

paper DOI: <https://doi.org/10.1021/acs.jmedchem.2c01446>

[View Online](#)

Toward CTPS1 inhibitors as a safer alternative to nucleoside chemotherapeutics: Rapidly growing cancer cells are critically dependent on synthesis of nucleotides, the building blocks of RNA and DNA. Blocking the synthesis of nucleotides is a tried-and-true mechanism of action for widely used chemotherapeutics such as cytarabine (ara-C) and gemcitabine. However, such molecules are toxic due to their non-specific activity. Cytosine 5'-triphosphate synthase (CTPS) 1 and 2 are homologous enzymes that catalyze the final step in the de novo synthesis of the nucleotide CTP from UTP. [Loss of CTPS1 function in humans](#) leads to increased susceptibility to infections due to inhibited B and T cell proliferation, suggesting its critical role in lymphoid cells.

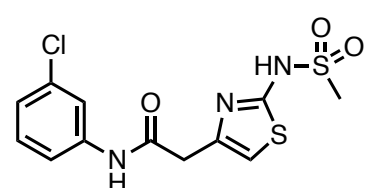
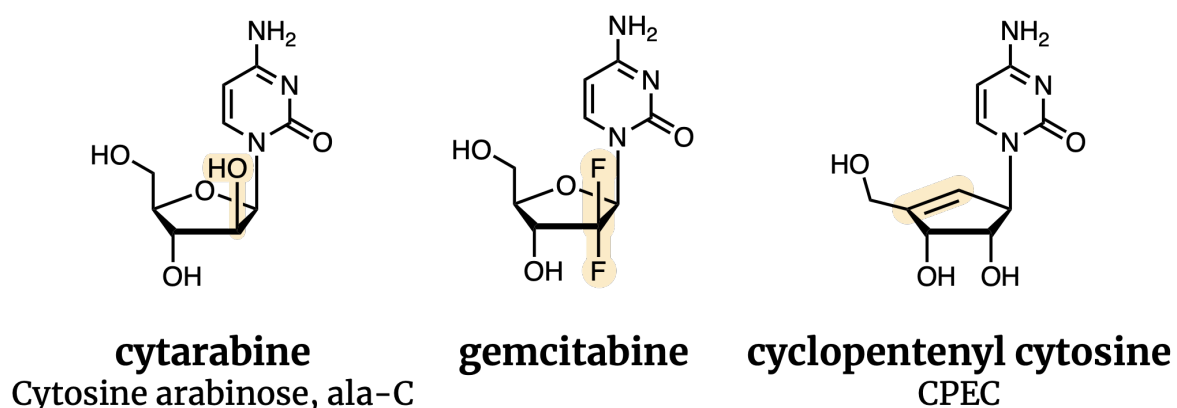
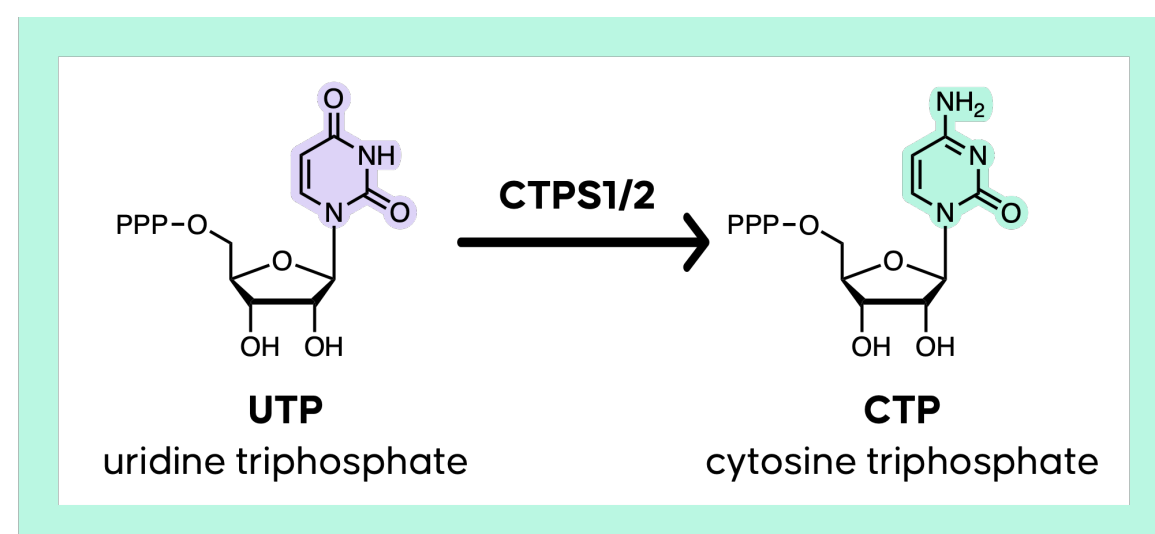
The lack of significant effects in non-hematopoietic cell lineages suggest CTPS2 activity is sufficient for proliferation of other cell types. Hence, CTPS1 might be a good target for immunology or blood cancers. To date, there have not been any CTPS1/2 inhibitors approved, though [cyclopentenyl cytosine](#) (CPEC) has been [clinically studied](#). Sygnature and Step Pharma ([founded by Kurma Partners and Sygnature](#)) set out to identify selective CTPS1 inhibitors, and appear to have been successful with Step Pharma's CTPS1-specific compound ([STP938](#), structure not disclosed) currently in a [Ph. I/II clinical study](#). The presently disclosed molecule, "[compound 27](#)" (T35) is a pan-selective inhibitor discovered en route to their desired CTPS1-selective molecule.

Lead generation. A biochemical HTS of a 240K compound library was run, confirming hits with dose-responses on hCTPS1 and four counterscreens for false positives and [PAINS](#), leading to "compound 1a" (2.3 μM). The acidic thiazole sulfonamide (pKa ~ 6.8) was critical for activity, as the less acidic amide and N-methylated sulfonamide derivatives were both inactive. Introduction of a cyclopropyl group increased biochemical potency, but a significant cell shift was seen in a [CTPS1-dependent cell line](#). Cellular potency was increased by masking the amide H-bond donor with an *ortho*-pyridyl moiety, increasing the overall lipophilicity of "compound 21". Finally, optimization against hepatic clearance, efflux, first-pass metabolism, and Ames toxicity was accomplished efficiently by adding only a few heavy atoms, resulting in "compound 27". CTPS2/1 selectivity was limited across species, and further efforts to optimize selectivity were not disclosed.

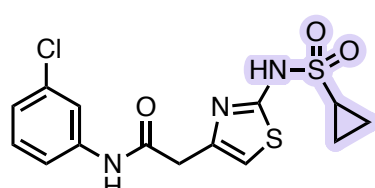
Binding mode and preclinical pharmacology: Cryo-EM (PDB:[7MIG](#)) and modeling confirmed that "compound 27" acts as a competitive CTPS1 inhibitor, binding in a pocket adjacent to the secondary CTP binding site. It demonstrated comparable efficacy to tofacitinib at 10 and 50 mg/kg PO BID in a [well-established arthritis mouse model](#) for inflammatory diseases. Exposures were dose-dependent, without time-dependent accumulation or activation of elimination pathways.

Patents: Composition of Matter and Preparation (Step Pharma S.A.S., France):

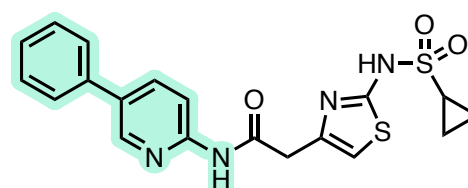
[WO2020245665](#) (10 December 2020), [WO2019106156](#) (06 June 2019), [WO2019106146](#) (06 June 2019), [WO2019179652](#) (26 September 2019).



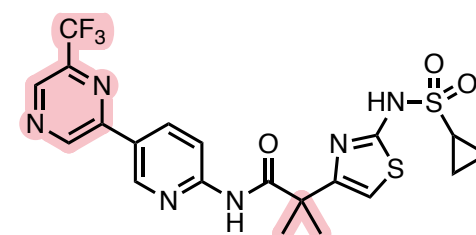
compound 1a
hCTPS1 IC₅₀ = 2.3 μM



compound 1e
hCTPS1 IC₅₀ = 0.25 μM
Jurkat IC₅₀ = 17 μM



compound 21
hCTPS1 IC₅₀ = 0.44 μM
Jurkat IC₅₀ = 4.8 μM



compound 27
FGFR3 IC₅₀ = 0.5 nM
FGFR1 IC₅₀ = 21 nM
BA/F3 IC₅₀ = 5.5 nM

compound 14d

β 2-AMPK

β 2-AMPK activator

in vivo efficacy in diabetic mouse model

scaffold hopping from MK-8722 + opt.

Bioorg. Med. Chem. Lett., 17 November 2022

SHIONOGI & CO., OSAKA, JP

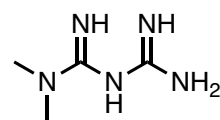
paper DOI: <https://doi.org/10.1016/j.bmcl.2022.129059>

[View Online](#)

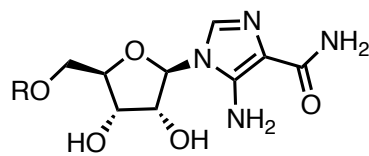
Revisiting AMPK activation with β 2-AMPK isoform potency.

“[Compound 14d](#)” (Shionogi & Co.) is a highly potent, dose-dependent [adenosine monophosphate activated protein kinase](#) (AMPK) activator being investigated for its blood-glucose-lowering effects. AMPK became a target-of-interest for the treatment of diabetes due to its role in regulating of glucose and lipid metabolism. Activation of AMPK switches on [catabolic pathways](#), [generates ATP](#), and ultimately inhibits gluconeogenesis. Indirect AMPK activators increase the AMP-ATP ratio, causing a conformational change and activation upon AMP binding to γ -subunits. AMPK is indirectly activated by one of the most widely prescribed drugs for Type 2 diabetes mellitus, [metformin](#) (Glucophage), with more than 92 million prescriptions filled in the US in 2020, making it the [third most-commonly prescribed medication](#). The different mechanism of indirect AMPK activation by metformin was recently reported, [inhibiting complex IV](#) instead of the assumed complex I inhibition, ultimately inhibiting hepatic gluconeogenesis. The exact mechanisms of other indirect [AMPK activators](#) including thiazolidinediones (TZDs), polyphenols, ginsenosides, or α -lipoic acid (ALA) are not well understood beyond the fact that they increase AMP-ATP ratios. While indirect AMPK activators are effective, more selective and direct activation of AMPK might lead to fewer off-target effects. The first class of direct AMPK activators and nucleoside-based diabetes treatments [AICAR and ZMP](#) (AICAR monophosphate) mimic cellular AMP and were FDA-approved in the 1990s.

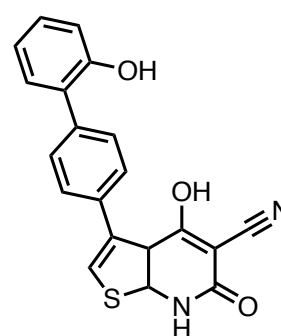
AMPK is an α,β,γ - heterotrimeric complex with a catalytic α -subunit (two isoforms) and regulatory β - and γ -subunits (two and three isoforms, respectively). The β 1-subunit is most predominantly expressed in the liver, whereas the β 2-subunit is exclusively expressed in skeletal muscle. In 2006, Abbott labs reported the first non-nucleoside small-molecule activator, [A-769662](#), which [uniquely binds](#) at the [allosteric drug and metabolite \(ADaM\) site](#). However, this [\$\beta\$ 1-selective compound](#) suffers from poor oral availability and permeability, as well as reported [off-target effects](#). β 1 and pan- β activators such as [MK-8722](#) and [PF-739](#) have been identified based on this binding site to help understand the role of β 2-specific effects, but the potencies of such molecules vs. β 2-AMPK complexes could be improved (generally >100 nM or micromolar activity). Studies using these molecules have suggested β 2 activation is required for glucose homeostasis, as supported by the established relationship between glucose uptake and an increase in the AMP/ATP ratio in [skeletal muscle](#) following exercise. “[Compound 14d](#)” was the result of a campaign to identify an activator with more potent activity on β 2-isoform-containing AMPK complexes.



Metformin
indirect AMPK activator



AICAR, R = H
ZMP, R = PO(OH)₂
AMP-mimetic, AMPK direct activator



A-769662
allosteric, non-nucleoside
direct AMPK activator

November 2022

compound 14d

β 2-AMPK

β 2-AMPK activator

in vivo efficacy in diabetic mouse model

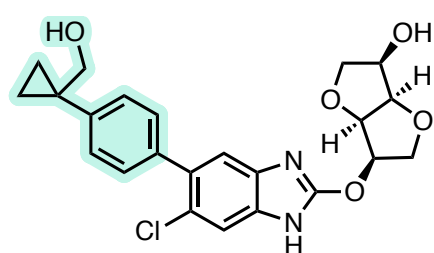
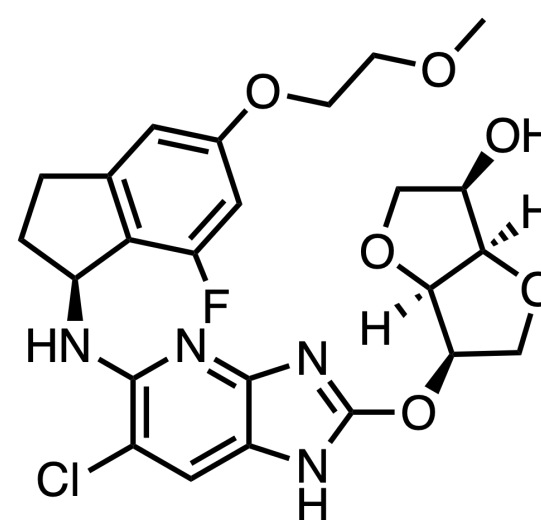
scaffold hopping from MK-8722 + opt.

Bioorg. Med. Chem. Lett., 17 November 2022

SHIONOGI & CO., OSAKA, JP

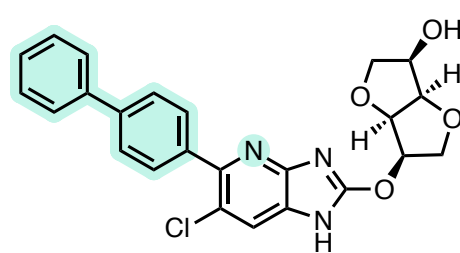
paper DOI: <https://doi.org/10.1016/j.bmcl.2022.129059>

[View Online](#)



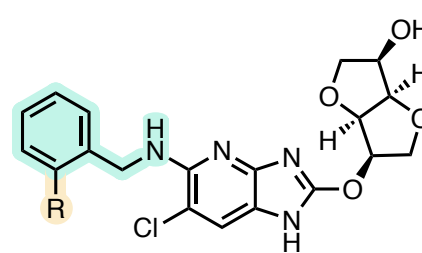
PF-739

AMPK (α 2 β 2 γ 3) EC₅₀ = 19 nM
AMPK (HSkM) EC₅₀ = 173 nM



MK-8722

AMPK10 (α 2 β 2 γ 1) EC₅₀ = ~10 μ M

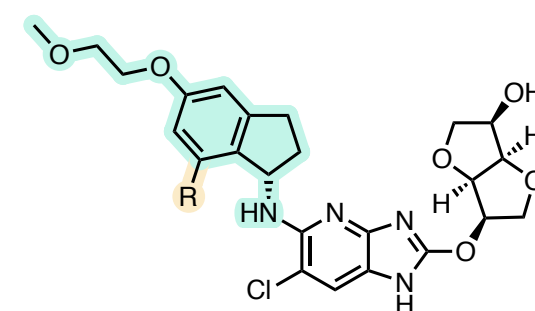


compound 12a (R = H)

AMPK (α 2 β 2 γ 1) EC₁₅₀ = 160 nM

compound 12c (R = F)

AMPK (α 2 β 2 γ 1) EC₁₅₀ = 48 nM



compound 14d (R = H)

AMPK (α 2 β 2 γ 1) EC₁₅₀ = 3.1 nM

compound 14d (R = F)

AMPK (α 2 β 2 γ 1) EC₁₅₀ = 1.6 nM

AMPK α 2 (L6GLUT4) EC₁₅₀ = 44.3 nM

From fragment-based screening to a new mechanistic hypothesis. “Compound 14d” was derived from scaffold hopping and optimization of a pan-AMPK activator reported by Merck in 2018. This activator, [MK-8722](#), was identified through optimization of a hit with micromolar activation of β 2 isoform-containing AMPK complexes in a fragment-based screen of ~25,000 compounds. Interestingly, the Merck series molecules exhibited significant distribution to the liver, with liver/muscle ratios of up to 650 being observed. Lower liver accumulation was important to see more potent β 2 activity in skeletal muscle.

Improving potency against β 2 isoform-containing AMPK complexes. Replacing the C5-biphenyl group of MK-8722 with a benzyl amine afforded “compound 12a” with 160 nM potency in a cell-free AMPK activity assay with a recombinant β 2 isoform. Potency jumped by an order of magnitude with an *o*-fluoro group on the benzyl ring (“12c”) or by two orders of magnitude with an (*S*)-aminoindane replacement of the benzyl amine (“13s”). Implementing these changes together and the addition of a 2-methoxyethoxy group on the 5-position of the aminoindane for improved cell-based performance resulted in “compound 14d” with EC₁₅₀ values of 1.6 nM (cell-free) and 44 nM (cell-based). “Compound 14d” was demonstrated to have no CYP metabolism liabilities (>20 μ M in

CYP1A2, 2C9, 2C19, 2D4 and 3A4), high protein binding (f_u = 3.1%), good microsomal stability (hMs = 91%, rMs = 81%), acceptable plasma concentrations (C_{max} = 65 ng/mL) and moderate clearance (CL_{tot} = 9.0 mL/min/kg).

Modest liver accumulation and desired skeletal muscle activity. Like MK-8722, “compound 14d” showed modest accumulation in the liver (~3.7x muscle K_p). In vivo efficacy studies with single oral dosing as low as 0.3 mg/kg in a diabetic (KKAY) mouse model demonstrated dose-dependent AMPK activation in skeletal muscle tissue and acute blood-glucose-lowering effects, while chronic dosing enabled dose-dependent suppression of hemoglobin A1c (HbA1c) elevation. In vivo glucose-lowering activity appeared to plateau at 3 mg/kg suggesting complete target engagement, though activity in skeletal muscle tissue increased with doses up to 5 mg/kg. Combined with previous results, these findings help confirm the β 2-isoform’s role in the glucose-lowering effects of AMPK activators.

November 2022

TDI-11861

sAC

oral sAC inhibitor

intended for male contraception

opt. from TDI-10229 + SBDD

J. Med. Chem., 08 November 2022

TRI-I TDI/WEILL CORNELL MEDICINE, NY

paper DOI: <https://doi.org/10.1021/acs.jmedchem.2c01133>

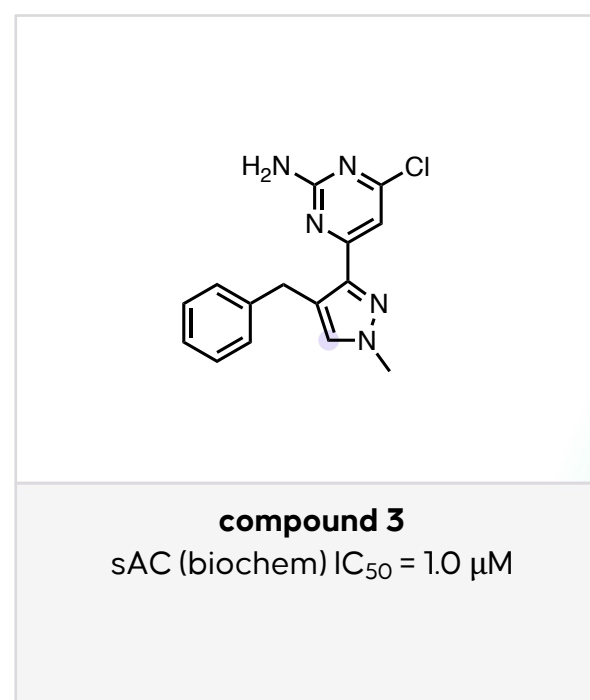
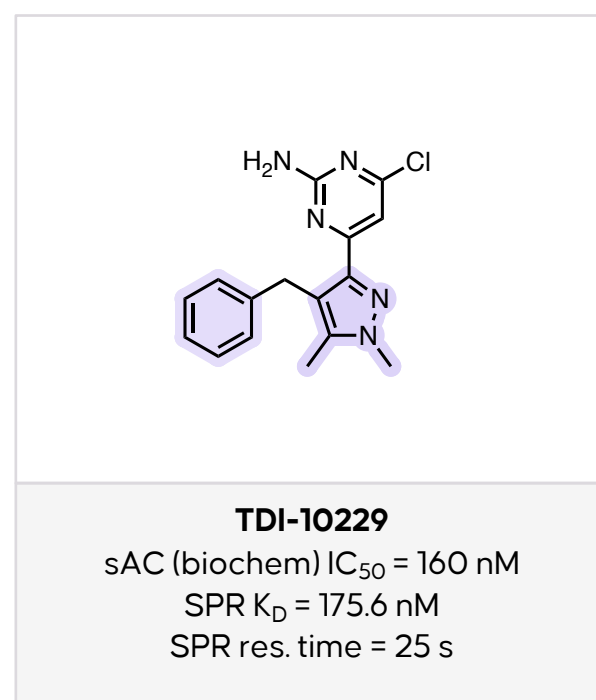
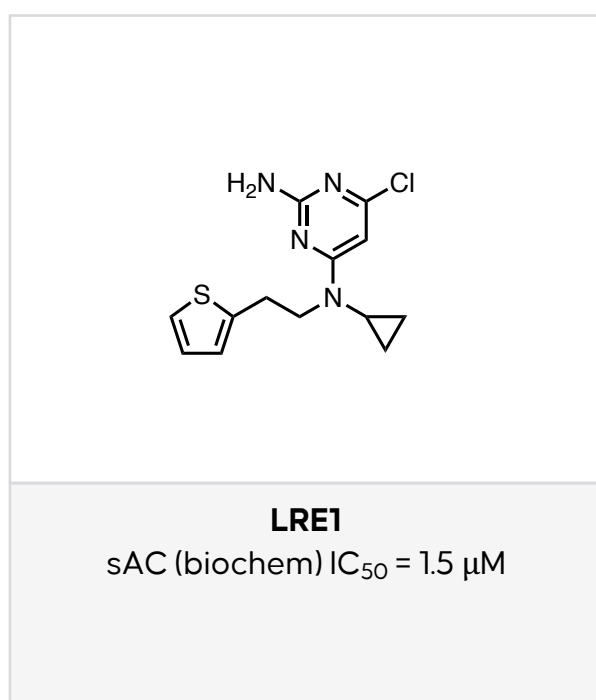
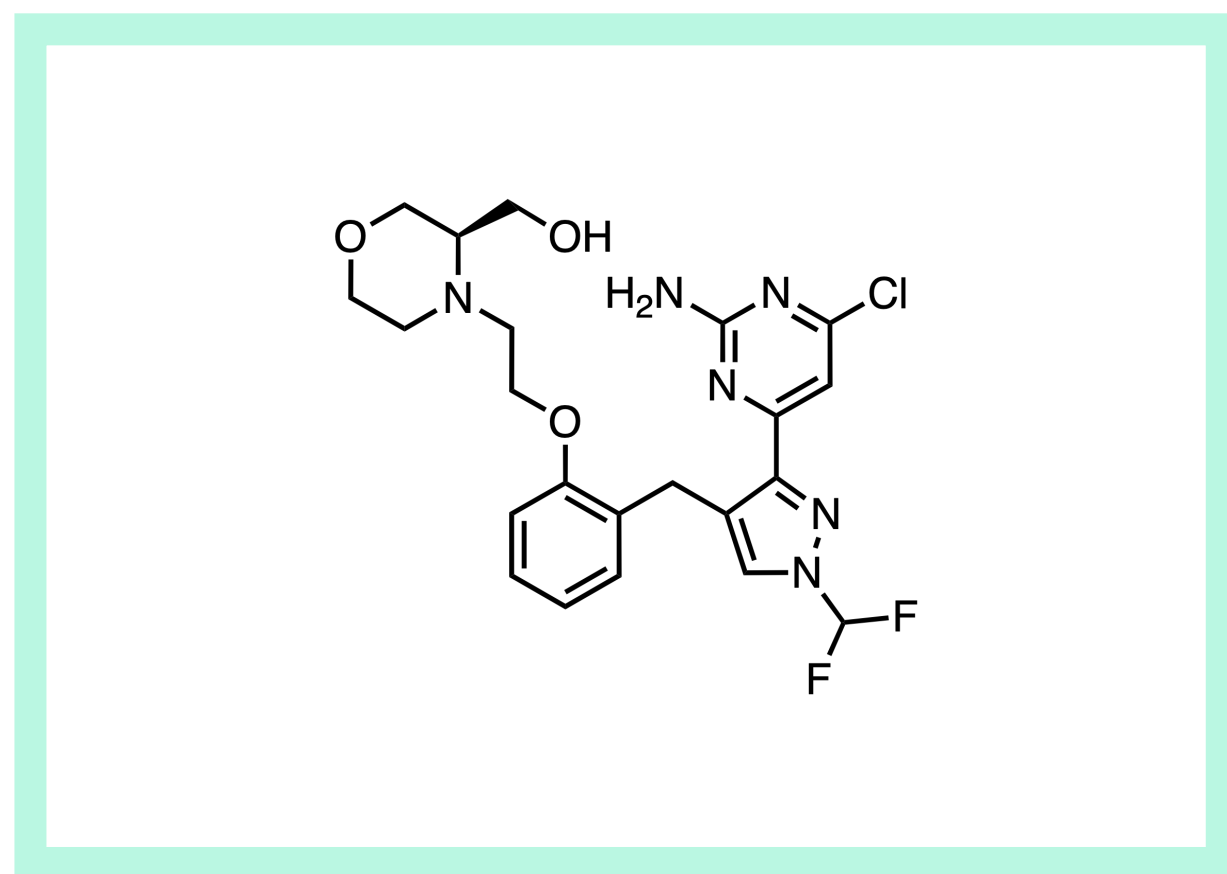
[View Online](#)

sAC as a target for male contraception. Soluble adenylyl cyclase (sAC) is [one of several ACs](#) that [catalyze the cyclization](#) of ATP to form cyclic adenosine monophosphate (cAMP). cAMP is the second messenger in [several signaling pathways](#) including that which activates sperm to be capable of fertilizing eggs (“[capacitation](#)”). The target is genetically validated in humans, as two adult human males were recently [diagnosed with infertility](#) due to a sAC mutation that rendered their sperm immotile. sAC inhibitors such as [TDI-11861](#) could be effective as on-demand, non-hormonal male contraceptives, a [longstanding unmet medical need](#).

Drug target residence time as a key property requirement.

sAC is [regulated by changes in cellular bicarbonate levels](#). Sperm are stored [under low bicarbonate conditions](#) (<5 mM), where sAC is inactive. Upon ejaculation, sperm are released into the seminal fluid, where

higher bicarbonate levels stimulate sAC, which activates sperm motility and initiates capacitation. In order to be effective, a sAC inhibitor would need to remain potent once the ejaculate is diluted upon deposition in the inhibitor-free female genital tract. While sAC is structurally similar to other ACs, its bicarbonate binding site is unique, providing an opportunity for selective inhibitor design. Earlier inhibitors from the Weill Cornell and TDI groups took advantage of this bicarbonate binding site, demonstrating moderate ([LRE1](#), $IC_{50} = 1,500$ nM) to modest ([TDI-10229](#), $IC_{50} = 160$ nM) potency in biochemical assays. However, these agents [did not provide adequate exposure](#) for use as a male contraceptive, likely due to their modest affinity and the dilutive effect of ejaculation upon entering the female genital tract. An inhibitor with a fast onset and slow dissociation rate was sought using TDI-10229 as a starting point.



November 2022

TDI-11861

sAC

oral sAC inhibitor

intended for male contraception

opt. from TDI-10229 + SBDD

J. Med. Chem., 08 November 2022

TRI-I TDI/WEILL CORNELL MEDICINE, NY

paper DOI: <https://doi.org/10.1021/acs.jmedchem.2c01133>

[View Online](#)

Increase in residence time via increased potency from structure-based design.

Analysis of the crystal structure of TDI-10229 bound to sAC (PDB:7QVD) hinted at a promising growth vector at the 5-position of the pyrazole; however, initial removal and/or substitution of the methyl groups significantly dropped affinity (e.g., “compound 3”). The use of [computational structure-based design tools](#) including free-energy perturbation (FEP) suggested that ortho substitution of the benzene ring may provide increased potency and was confirmed by the addition of a methyl ether (“compound 11”). Modeling further predicted that extension of the ortho substituent on the benzene with an alkyl chain with a hydrophobic or weakly basic moiety would be productive (“compound 19”). The potentially metabolically unstable pyrazole *N*-methyl group was replaced with a gem-difluoromethyl group (“compound 23”), accompanied with a small increase in potency. Addition of a hydroxymethyl moiety to the morpholine resulted in TDI-11861 (PDB:8B75), now with significantly greater potency and residence time than TDI-10229.

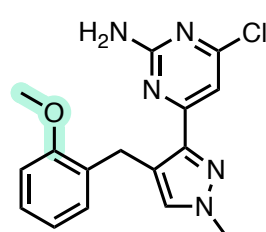
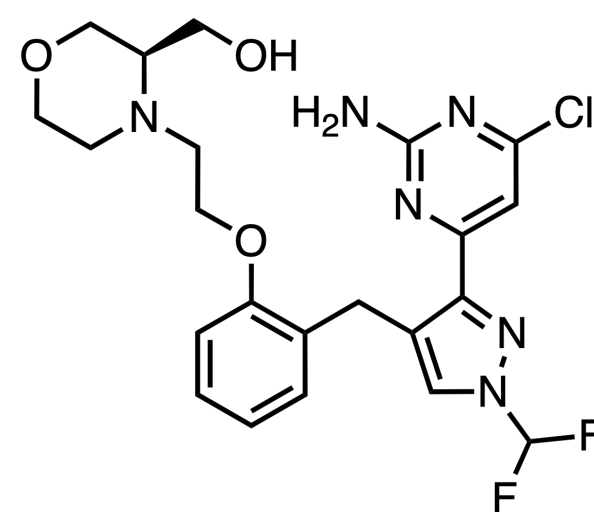
A jump dilution recovery assay to verify slow dissociation.

To mimic what happens upon the deposition of sperm into the female reproductive tract, a [jump dilution recovery assay](#) was performed. In the assay, the inhibitor is preincubated with sAC at 5X its standard assay concentration. After 15 minutes, the inhibitor-protein solution is diluted 100-fold; cyclase activity is initiated and then measured at regular intervals. Compounds with

short residence times will lose their inhibitory activity quickly, but those with longer residence times will retain activity, albeit decreased until the inhibitor ultimately dissociates from the protein. The time it takes to lose activity is then defined as the inhibitor’s residence time. For TDI-11861, the residence times measured in the SPR (3,181 s) and jump dilution (1,220 s) are in reasonable agreement, with the variance explained by differences in assay conditions.

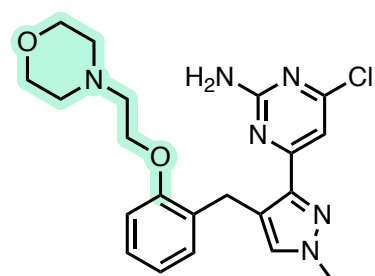
A promising compound profile for TDI-11861:

TDI-11861 showed good overall PK in CD-1 mice. Although oral bioavailability was low when dosed at 10 mg/kg (%F = 11), unbound plasma exposures of ~10-fold over the cellular IC₅₀ (5.5 nM) could be obtained when dosed at 50 mg/kg. PAMPA studies showed good membrane permeability (463 nm/s), with a solubility of 79 µg/mL. Furthermore, TDI-11861 had high selectivity for sAC over the related tmAC family members and did not show significant activity against a panel of 322 kinases or 46 other targets in a Eurofins safety panel (e.g., GPCRs, ion channels, nuclear receptors). No cytotoxicity was observed at 20 µM, nor was there glutathione adduct formation in a 2 hr trapping study, despite the presence of the potentially reactive chloropyrimidine. The molecule does not appear to be in clinical development, and it is not clear that the longer residence time or drug safety is sufficient yet for clinical application. TDI-11861 and related sAC inhibitors have been described in the patent [WO2022232259A1](#), though no US patents have been disclosed.



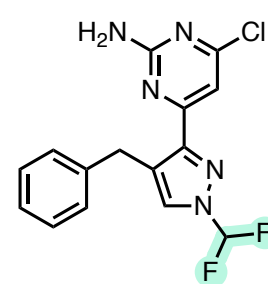
compound 11

sAC (biochem) IC₅₀ = 67 nM



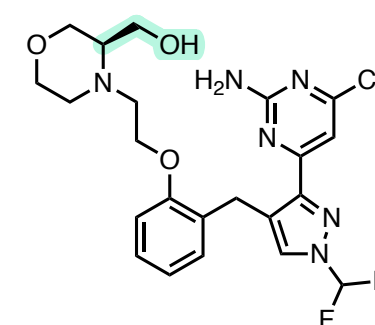
compound 19

sAC (biochem) IC₅₀ = 12.3 nM
SPR res. time = 1,378 s
jump dil. res. time = 542 s



compound 23

sAC (biochem) IC₅₀ = 3.9 nM
sAC (cell) IC₅₀ = 1.9 nM
SPR K_D = 3.3 nM
SPR res. time = 1,832 s



TDI-11861

sAC (biochem) IC₅₀ = 3.3 nM
sAC (cell) IC₅₀ = 5.5 nM
SPR K_D = 1.4 nM
SPR res. time = 3,181 s
jump dil. res. time = 1,220 s

November 2022

EG-011

WASp

WASp activator

in vivo antitumor activity

fortuitous scaffold hopping from ibrutinib

bioRxiv, 25 November 2022

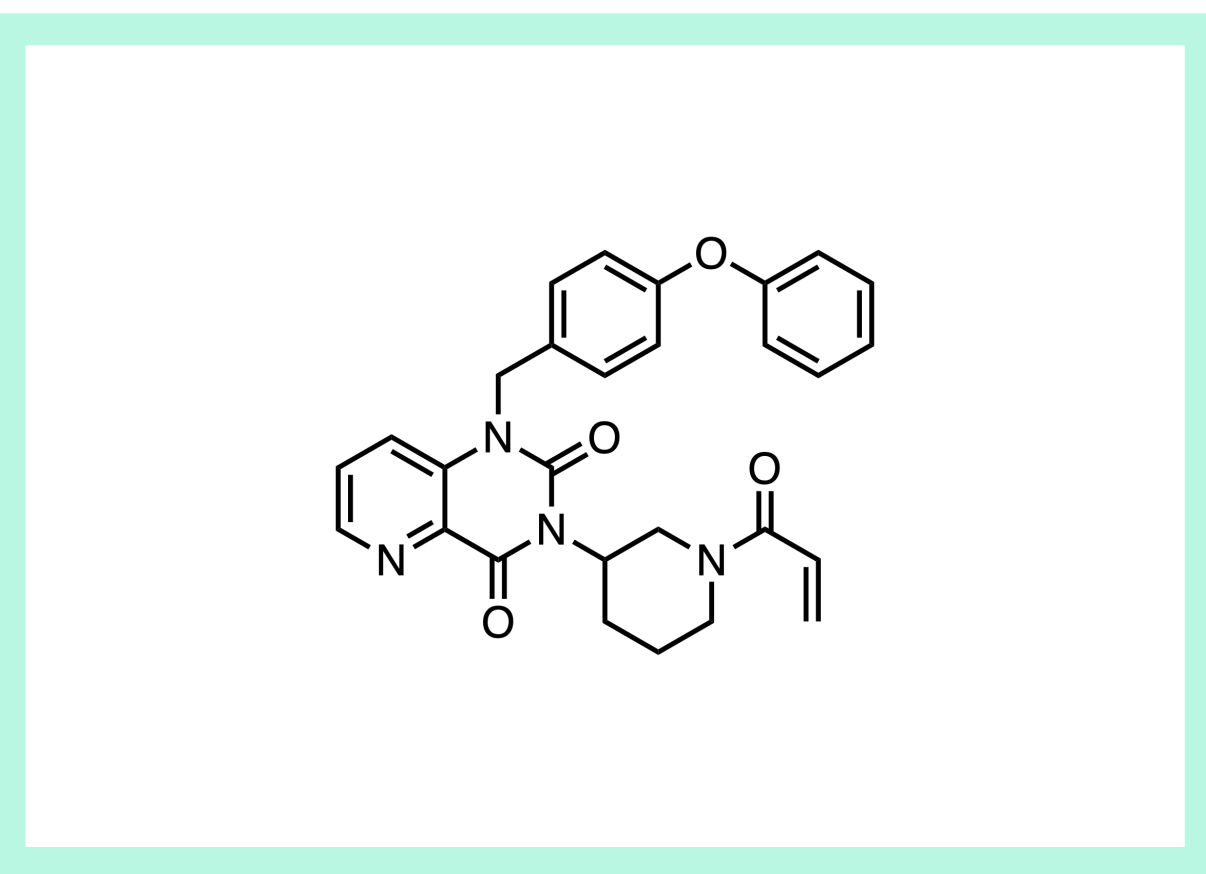
INSTITUTE OF ONCOLOGY RESEARCH, CH

paper DOI: <https://doi.org/10.1101/2022.11.25.517686>

[View Online](#)

WASp as a new target for hematological cancers. Wiskott-Aldrich syndrome protein ([WASp](#)) is a protein almost exclusively expressed in hematopoietic cells that promotes actin polymerization. The WAS gene plays an important but not fully understood role in human immune cell biology, illustrated by [WASp deletion in B-cells inducing autoimmunity](#) in WAS patients or [15% of patients with WAS mutations developing lymphoma](#) in another study. Small molecules have been reported to modulate WASp function, as demonstrated by the elucidation of [wiskostatin](#)'s WASp inhibition MOA or the antiproliferative activity of the WASp degradation promoter, [SMC #13](#), in lymphoma and leukemia models. However, tools for understanding WASp biology are still limited. WASp is [phosphorylated by a variety of kinases](#) resulting in different effects, including BTK. Interestingly, while preparing analogs of the BTK inhibitor, ibrutinib, the Swiss Institute of Oncology Research serendipitously discovered a molecule without kinase inhibition activity that appears to be the first small molecular activator of WASp, [EG-011](#).

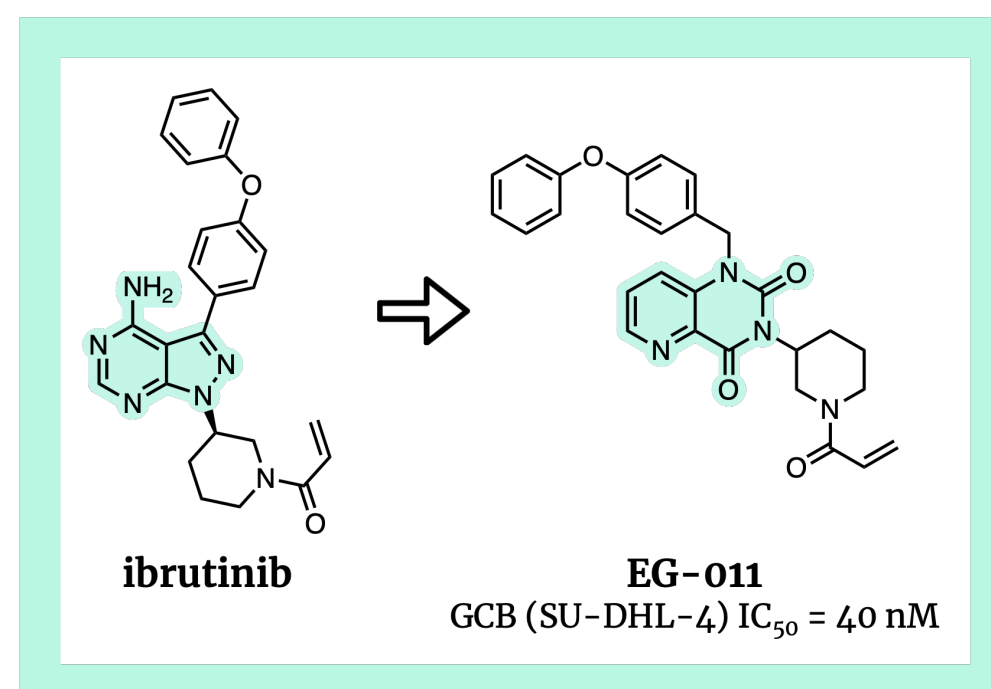
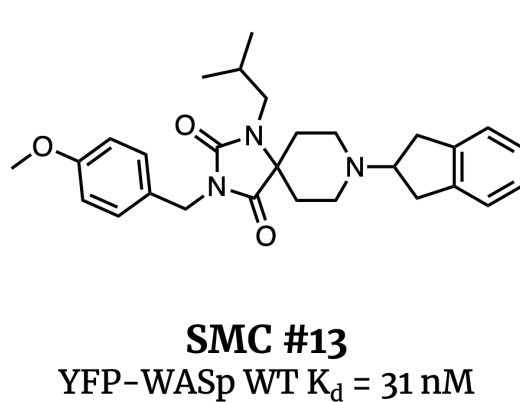
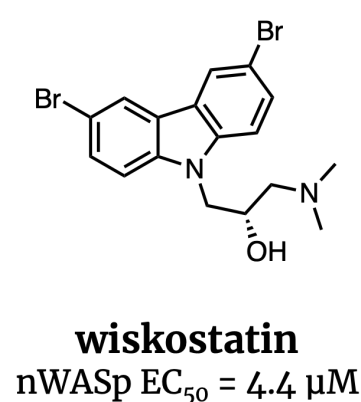
Serendipitous discovery of WASp activator without kinase activity from a scaffold hop of a BTKi. EG-011 was the result of modification of the central aminopyrazolopyridimine core of the BTKi, [ibrutinib](#), to a pyridylpyrimidione. EG-011 has activity in various hematopoietic cancer cell lines, but EG-011's activity is not due to kinase inhibition, as confirmed by the lack of activity in KINOMEScan (450 kinases + mutants) or PanKinase activity assays (radiometric assay, 320 kinases). This should not be surprising to chemists, as this small change removes the critical hinge-binding element of ibrutinib. In a thermal proteome profiling (TPP) experiment with EG-011-treated REC-1 cells, WASp was the most highly destabilized protein, along with 47 additional potential targets identified, 8 of which were stabilized protein interactions. The proposed mechanism of WASp



activation was further confirmed by the acceleration of actin polymerization with EG-011 in the presence of autoinhibited WASp ($t_{50} = \sim 1$ ks, vs. 2.5 ks without EG-011), and lack of activity in the absence of this construct, even at 10 μ M EG-011. In contrast, a weaker effect on actin polymerization was seen when constitutively active WASp was used, supporting the activation mechanism. Fluorescence imaging further confirmed an increase in actin polymerization in an EG-011-sensitive cell line, with an increase in number of high intensity filamentous actin spots, as well as overall amplified fluorescence signal. The transcriptome profile of EG-011 was most similar to microtubule-stabilizing agents, such as taxanes, or HDAC inhibitors, which eventually lead to cell death in all cases.

Promising in vitro data recapitulated during in vivo experiments. EG-011 demonstrated single-digit micromolar antitumor activity via cell death induction against lymphomas (GCB, DLBCL, MCL, MZL) and acute lymphoblastic leukemia (ALL), but not other acute leukemia or solid tumor cell lines. The compound maintained or even increased potency in models of secondary resistance to PI3K/BTK inhibition (MZL cell lines) or proteasome inhibition (MM models). Additive or synergistic efficacies were observed in combination treatments with rituximab, venetoclax, ibrutinib or lenalidomide in EG-011-sensitive DLBCL or MCL cell lines. Finally, the in vivo antitumor activity of EG-011 was demonstrated in a mouse xenograft model (REC1 MCL cell line) with 2.2-fold reduction in tumor size following 200 mg/kg QD dosing for 9 days, without significant signs of toxicity.

Patent. "New compounds with antitumor effects" [WO2019185117A1](#) (03 October 2019)



Past Molecules

Hall of Fame

2022

[01 January](#)

[02 February](#)

[03 March](#)

[04 April](#)

[05 May](#)

[06 June](#)

[07 July](#)

[08 August](#)

[09 September](#)

[10 October](#)

2021

[01 January](#)

[02 February](#)

[03 March](#)

[04 April](#)

[05 May](#)

[06 June](#)

[07 July](#)

[08 August](#)

[09 September](#)

[10 October](#)

[11 November](#)

[12 December](#)

2020

[02 February](#)

[03 March](#)

[04 April](#)

[05 May](#)

[06 June](#)

[07 July](#)

[08 August](#)

[09 September](#)

[10 October](#)

[11 November](#)

[12 December](#)

Yearly Nominees

[2020](#)

[2021](#)

Yearly Winners

[2020](#)

[2021](#)

Thank You!

Try Premium.

and gain access to hundreds more molecule reviews like this, plus content like:

**Drug Approvals • Tech Reviews • IPO and M&As,
and more features like our sub-structure search.**

sign up for a trial today at <https://drughunters.com/3WsorHv>

info@drughunter.com